Chapter 17

Random Motion, Molecular and Turbulent Diffusivity

17.1 Random Motion
Random Walk
Solutions of the Time-Dependent Diffusion Equation

17.2 Molecular Diffusion
The Complex Nature of Molecular Diffusion Processes
Diffusion Coefficients in Air
Diffusion Coefficients in Water
Molecular Diffusivities in Porous Media
Diffusion of Sorbing Chemicals in Porous Media: Effective Diffusivity
Box 17.1 Diffusive Transport of Sorbing Chemicals in Sediments and Saturated Soils: Effective Diffusivity

17.3 Other Random Transport Processes in the Environment
Turbulent Diffusion
Diffusion Length Scales
Measurement of Vertical Turbulent Diffusivity
Box 17.2 Calculating Vertical Turbulent Diffusivity from Radon Diffusion in Lakes and Oceans
Dispersion

17.4 Questions and Problems

17.5 Bibliography

Environmental Organic Chemistry, Third Edition. René P. Schwarzenbach, Philip M. Gschwend, and Dieter M. Imboden.
Copyright © 2017 John Wiley & Sons, Inc. Published 2017 by John Wiley & Sons, Inc.
Companion website: www.wiley.com/go/Schwarzenbach/EnvironmentalOrganChem3e

To describe the fate of organic chemicals in environmental systems under the simultaneous influence of transformation and transport processes, mathematical models of increasing complexity were derived in Chapter 6. The first and simplest model discussed in Chapter 6, the box model, did not include internal mixing. Instead, the only mechanisms involving transport were the exchanges of the chemical across the boundaries of the boxes, the input and output processes. In this chapter, we deal with the effect of random motion on transport processes in the environment. Random motion occurs on the molecular level, reflecting the physics at the atomic scale, and it characterizes the turbulent flow of fluids (gas or liquid). In every case, the mathematics looks the same, as the chemical flux caused by random motion is equal to the intensity of the random motion multiplied by the chemical gradient in space. The goals of this chapter are to understand how the intensity of the random motion translates into values of the molecular or eddy diffusivities and how, in particular situations, we can solve for chemical fluxes produced by random motion.

In Section 17.1, the theory of random motion is presented, its relation to the normal or Gaussian distribution is derived, and the resultant concentration changes and mass fluxes for characteristic physical situations are presented. In Section 17.2, we discuss molecular diffusion of organic chemicals in the most important environmental media: air and water. Section 17.3 deals with turbulent diffusion and dispersion.

17.1 Random Motion

In Section 6.3, using the example of a cup of coffee in a dining car of a train (A Thought Experiment in a Train), we showed that transport processes in natural systems result from the superposition of random and directed processes. The distinction between the two depends on the scale of resolution at which we are analyzing transport processes. In this chapter, we focus on the "fine structure" of transport where motion becomes random. Transport by random motion is called diffusion.

Random Walk

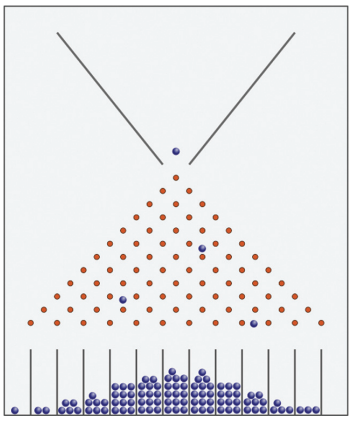

Galton Box. Graphic: Floryan (2007).

The movement of a particle (e.g., molecule, sand grain, bacterial cell) due to random processes is called a random walk. A well-known example is the Brownian motion named after the botanist Robert Brown, who in 1827 observed the irregular motion of pollen grains suspended in water. Nearly a century later, Albert Einstein explained Brown's observation as the result of water molecules colliding with the pollen grains. One consequence of Einstein's theory is Eq. 6-36, the Einstein-Smoluchowski law (Einstein, 1905), stating that the mean distance of transport by diffusion grows as the square root of time, in contrast to transport by advection in which distance grows linearly with time.

Binominal Distribution. As an illustration of the Einstein-Smoluchowski law, we use the so-called Galton Box, a classic toy made of pegs fixed on an inclined board. A ball starts from the top of the board at $x = 0$ and, rolling down the slope, has a 50 percent chance to move either to the right (positive x-axis) or to the left (negative x-axis) every

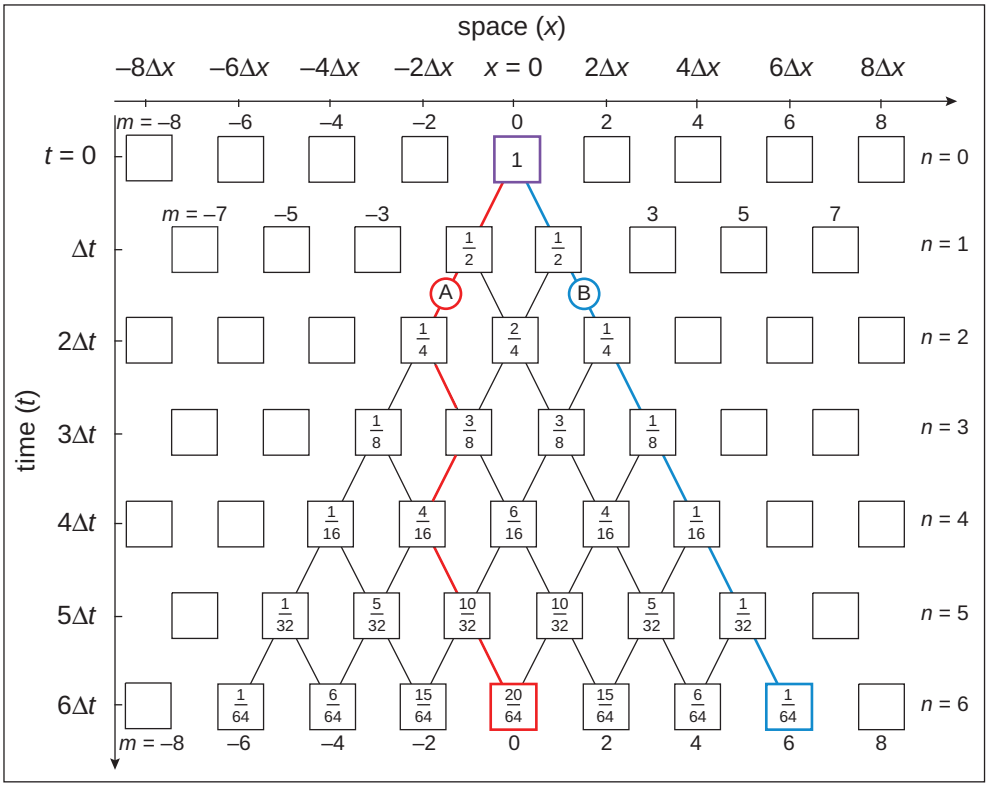

Figure 17.1 Random walk of a ball through an array of pegs. At each peg (represented by a square), the ball has equal chance to move to the right or left. The numbers in the boxes give the probability, $p(n,m)$, for an individual ball to reach this box. Drawn in color are examples of individual particle tracks (A and B). The probability to reach the center box, like A, is 20/64, while the probability to arrive at the box farthest to the right, like B, is 1/64.

time it hits a peg. In Fig. 17.1, the pegs are depicted as squares with a fraction that gives the probability that an individual ball arrives at each peg. If the layers of pegs are equally spaced along the slope, the vertical axis can also be interpreted as the time axis measuring the elapsed time since the beginning of the ball's journey, $t = n\ \Delta t$, where n is the number of hits with a peg, and Δt the time between hits.

The path of an individual ball cannot be predicted, but if a large number of balls has moved down the slope and is collected along the x-axis after a certain number of hits, a symmetric distribution of balls will emerge called the binominal distribution with its maximum at the center ($x = 0$). The longer the journey of the balls, that is, the larger the number of hits and of elapsed time, the broader is the distribution of balls along the x-axis. The probabilities for a ball to reach a particular peg m after n hits, $p(n,m)$, is given by:

$$p(n,m) = \frac{n!}{2^n \left[\frac{1}{2}(n-m)\right]! \left[\frac{1}{2}(n+m)\right]!};$$
$$m = -2n, -2(n-1), \ldots +2(n-1), +2n \qquad (17\text{-}1)$$

where $n! = 1{\cdot}2{\cdot}3 \ldots (n{-}1)n$ is n-factorial. Figure 17.2 shows $p(n,m)$ for $n = 6$ (6 hits). The values of m run only through even or odd numbers depending on whether n is even or odd. Since at every layer of pegs the probability that a ball hits one of the pegs in that layer must be one, for a given layer n, the sum of $p(n,m)$ with either even or odd m-values is one.

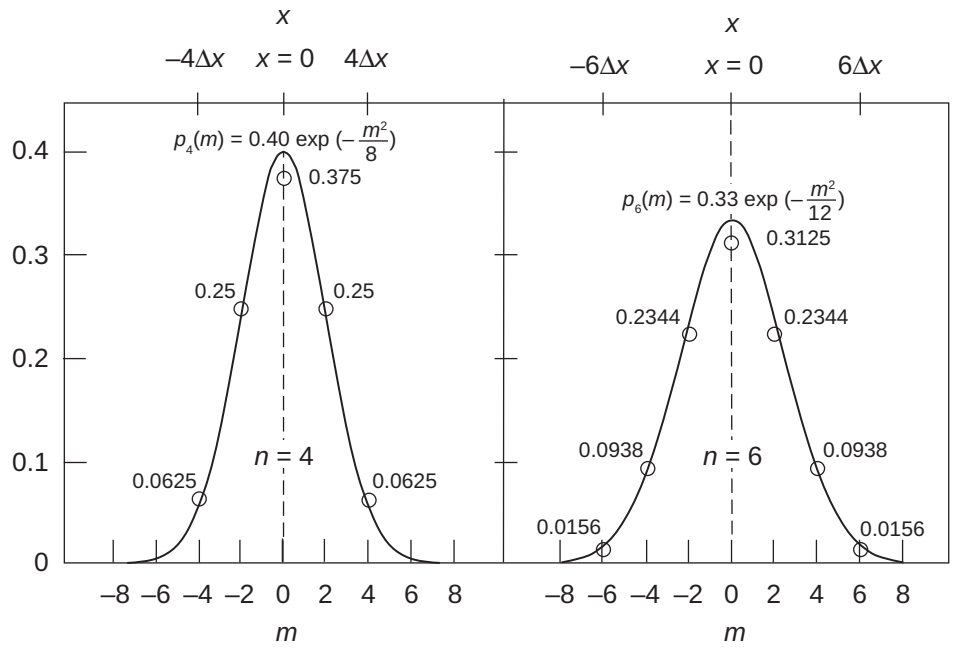

Figure 17.2 Coefficients of the binominal distribution, $p(n,m)$, for $n = 4$ and $n = 6$ (open circles with numbers) compared to the continuous approximation by de Moivre and Laplace, $p_n(m)$.

To evaluate Eq. 17-1 for large values of n is quite cumbersome. Fortunately, the French mathematicians, de Moivre and Laplace, found that with increasing n, $p(n,m)$ converges to the function:

$$p(n,m) \rightarrow p_n(m) = \left(\frac{2}{\pi n}\right)^{1/2} \exp\left\{-\frac{m^2}{2n}\right\} \tag{17-2}$$

As shown in Fig. 17.2, the approximation of $p(n,m)$ by the continuous function $p_n(m)$ is quite good, even for small n-values.

Normal Distribution. The function $p_n(m)$ is a one-dimensional normal (or Gaussian) distribution along the m-axis with maximum at $m = 0$. The subscript n characterizes the shape of the distribution: the larger the n, the broader the distribution and the smaller its maximum (see Fig. 17.2). The normal distribution is important in many fields of science, appearing wherever random processes are at work. Usually, it is written as a function of the general coordinate x, $p_\sigma(x)$:

$$p_\sigma(x) = \frac{1}{(2\pi)^{1/2}\sigma} \exp\left(-\frac{x^2}{2\sigma^2}\right) \tag{17-3}$$

The standard deviation, σ, defines the width of the distribution and, thus, corresponds to the "shape parameter" n of Eq. 17-2. Important properties of the normal distribution are summarized in Appendix A.1.

In order to find the relation between the approximate representation of $p(n,m)$ by de Moivre and Laplace (Eq. 17-2) and the normal distribution (Eq. 17-3), we relate the parameters n and m to time t and spatial distance x by introducing two quantities that

are important for the theory of molecular motion. The first is the mean free path, λ, and the second is the mean velocity of the molecule between consecutive hits, $\overline{u}_x$. Using the definitions introduced in Fig. 17.1, we get $\lambda = \Delta x$ and $\overline{u}_x = \Delta x/\Delta t = \lambda/\Delta t$. With $m = x/\Delta x$ and $n = t/\Delta t$, the argument of the exponential function of Eq. 17-2 can then be expressed as:

$$\frac{m^2}{2n} = \frac{1}{2}\frac{x^2}{\lambda^2}\frac{\lambda}{\overline{u}_x t} = \frac{1}{2}\frac{x^2}{\lambda \overline{u}_x t} \tag{17-4}$$

By comparing this result with Eq. 17-3, we get the following relation between the standard deviation, σ, and the two quantities that characterize the random walk, λ and $\overline{u}_x$:

$$\sigma = (\lambda \overline{u}_x t)^{1/2} \tag{17-5}$$

Equation 17-5 is similar to the Einstein-Smoluchowski law (Eq. 6-36), particularly to its property that diffusion distance grows as $t^{1/2}$, in contrast to advection where distance grows linearly with time. If we take σ as the diffusive transport distance, L_{diff}, the equivalence of the two expressions, Eq. 6-36 and 17-5, yields the following relationship between diffusivity, D, and random walk parameters:

$$D = \frac{1}{2}\lambda \overline{u}_x \tag{17-6a}$$

If this expression is extended to three dimensions, the numerical factor on the right-hand side of Eq. 17-6*a* becomes 1/3 (Jeans, 1921):

$$D = \frac{1}{3}\lambda \overline{\boldsymbol{u}} \tag{17-6b}$$

where $\overline{\boldsymbol{u}}$ is the average molecular speed in the three-dimensional space.

Solutions of the Time-Dependent Diffusion Equation

We now show that the normal distribution is a solution of Fick's second law:

$$\frac{\partial C}{\partial t} = D\frac{\partial^2 C}{\partial x}; \quad D = \text{constant along } x\text{-axis} \tag{6-34b}$$

and that the diffusion coefficient D is indeed related to the standard deviation as stated by the Einstein-Smoluchowski law (Eq. 6-36). Generally, the solutions of Eq. 6-34*b* are exponential functions or integrals of exponential functions such as the error function (see Eq. 17-9 and Appendix A.2). These solutions depend on the boundary conditions and initial condition. The initial condition is the concentration distribution along the x-axis at a given time which is conveniently chosen as $t = 0$. The boundary conditions can be defined in different ways. For instance, the concentration may be held fixed at a "wall" located at $x = 0$, or it may harmonically oscillate around a mean value. In many cases, solutions are found only by numerical approximations. The mathematical techniques for the solution of the diffusion equation (such as the

Laplace transformation) are extensively discussed in Crank (1975) and Carslaw and Jaeger (1959).

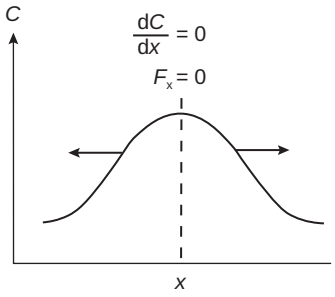

Symmetric diffusion.

Symmetric Diffusion from an Initial Infinitely Sharp Concentration Peak. As a first application of Fick's second law, we consider the symmetric propagation of a chemical with total mass $\mathcal{M}^*$ per unit area (dimension ML^{-2}) into infinite space ($x \to \pm\infty$). At time $t = 0$, this compound is all concentrated at $x = 0$. The function which is infinite at $x = 0$ and zero otherwise but has a finite integral is the *delta function* defined by:

$$\delta(x) = \begin{cases} 0 & \text{for } x \neq 0 \\ \infty & \text{for } x = 0 \end{cases} \quad \text{with} \int_{-\infty}^{+\infty} \delta(x) = 1 \tag{17-7}$$

As can be shown by inserting into Eq. 6-34*b*, the following function is a solution that obeys the required initial and boundary conditions (i.e., for $t \to 0$, it converges to the delta function centered at $x = 0$ and drops to zero for $x = \pm\infty$):

$$C(x,t) = \frac{\mathcal{M}^*}{2(\pi Dt)^{1/2}} \exp\left(-\frac{x^2}{4Dt}\right) \quad [ML^{-3}] \tag{17-8}$$

Equation 17-8 is a normal distribution (Appendix A.1) with standard deviation $\sigma_x = (2Dt)^{1/2}$. From a mathematical point of view, the initial condition of the previous example is equivalent to the situation of the peg board where all the balls enter the system at $x = 0$. Now, everything falls into place. The process of random motion transforms a "point source" (like molecules initially all located at $x = 0$, or balls all entering a peg board at one location) into a normal distribution whose standard deviation, σ, grows like $(2Dt)^{1/2}$, in accordance with the Einstein-Smoluchowski law.

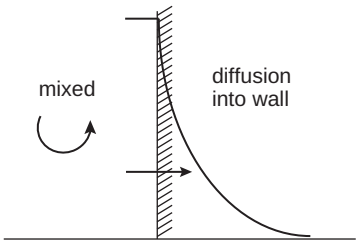

One-sided diffusion from boundary.

One-Sided Diffusion from a Boundary. As a second example, we apply Fick's second law (Eq. 6-34*b*) to the case of one-dimensional diffusion between two systems separated by a boundary located at $x = 0$ (Fig. 17.3*a*). System 1 is located left of the boundary ($x < 0$), and system 2 is to the right of the boundary ($x > 0$). The concentration of a chemical in system 1, including the boundary at $x = 0$, is held constant with time at the initial value, $C_1^0 > 0$. We use subscripts to denote the system (system 1, system 2) and superscripts to mark initial values ("0") or steady-state values ("∞"). The initial value in system 2 is $C_2^0(x > 0) = 0$. At $t = 0$, the chemical starts to diffuse from the boundary into system 2.

The solution of Eq. 6-34*b* with these initial and boundary conditions is (see Crank, 1975):

$$C_2(x,t) = C_1^0 \text{erfc}\left(\frac{x}{2(Dt)^{1/2}}\right) \quad \text{for } x \geq 0 \tag{17-9}$$

The expression, erfc(y), is called the complementary error function for the argument $y = \frac{x}{2(Dt)^{1/2}}$ (see Appendix A.2). The function steadily decreases from its value at $y = 0$, $\text{erfc}(0) = 1$ to its value at $y = \infty$, $\text{erfc}(\infty) = 0$, but most of the drop occurs between $y = 0$ and 1 ($\text{erfc}(1) = 0.158$).

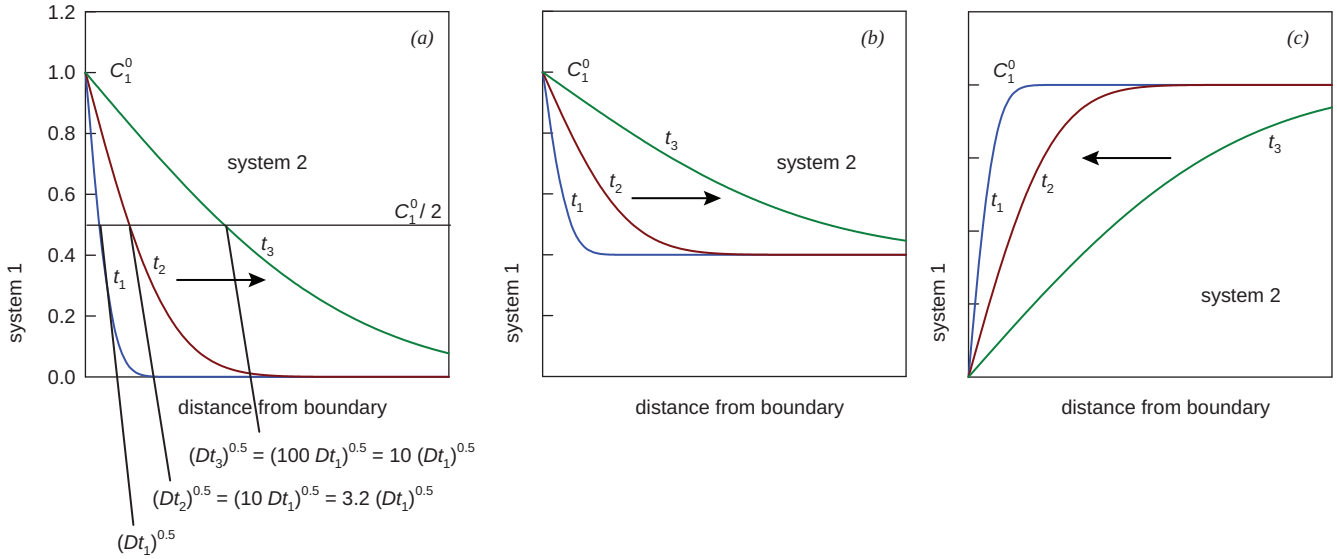

Figure 17.3 Solution for the time-dependent diffusion equation (Fick's second law, Eq. 6-34*b*) for one-sided diffusion from a boundary with constant concentration, C_1^0, into the semi-infinite space (Eq. 17-9) for different initial conditions. (*a*) $C_1^0 = 1$, $C_2^0 = 0$; (*b*) $C_1^0 = 1$, $C_2^0 = 0.4\,C_1^0$; (*c*) $C_1^0 = 0$, $C_2^0 > 0$. As indicated by the arrows, for (*a*) and (*b*), diffusive transport is from the boundary into system 2, and for (*c*), it is from system 2 to the boundary. The three consecutive times are related by $t_2 = 10\,t_1$, $t_3 = 100\,t_1$. In (*a*), the half-concentration penetration distance is shown.

Now, we ask how fast does a "concentration front" move along the positive x-axis if at time $t = 0$ the semi-infinite system 2 is suddenly exposed to a boundary concentration C_1^0? Let us agree that we identify the front by the position of half the boundary value, $C_1^0/2$, and that we call the location of that specific choice the half-concentration penetration distance, $x_{1/2}$. To calculate $x_{1/2}$ as a function of time, we need to find the y-value for which erfc(y) becomes equal to 0.5. We call this value $y_{1/2}$. Thus, we have the following implicit equation: $\text{erfc}(y_{1/2}) = 0.5$. According to Appendix A.2, $y_{1/2} = 0.48$; therefore, in Eq. 17-9, the argument of erfc must be equal to $y_{1/2} = 0.48$:

$$\frac{x_{1/2}}{2(Dt)^{1/2}} = y_{1/2} = 0.48 \tag{17-10}$$

Solving for the half-concentration penetration distance yields:

$$x_{1/2} = 2y_{1/2}(Dt)^{1/2} = 0.96(Dt)^{1/2} \approx (Dt)^{1/2} \tag{17-11}$$

As in other diffusive situations, the penetration distance grows as $t^{1/2}$.

We may also ask how much of the chemical has crossed the boundary at time t? To calculate the total mass flux per unit boundary area after elapsed time t, $\mathcal{M}^*(t)$, we integrate the concentration profile of Eq. 17-9 from $x = 0$ to $x = \infty$. With Eq. (4) of Appendix A.2, we get:

$$\mathcal{M}^*(t) = C_1^0 \int_0^\infty \text{erfc}\left(\frac{x}{2(Dt)^{1/2}}\right) \mathrm{d}x = \frac{2}{\sqrt{\pi}} C_1^0 (Dt)^{1/2} = 1.13\ C_1^0 (Dt)^{1/2} \quad [\text{ML}^{-2}] \tag{17-12}$$

Again, the integrated mass that has crossed the boundary grows as $t^{1/2}$.

Since Fick's diffusion equations are linear, Eqs. 17-9 to 17-12 remain valid if a fixed value is added to or subtracted from concentration C. For instance, let us assume that the initial concentration right of the boundary (system 2) is different from zero, say $C_2^0 = 0.4C_1^0$ (Fig. 17.3*b*). In order to arrive at the same situation as before, we introduce new concentrations, C_1^* and C_2^*, by subtracting the constant value C_2^0 from C_1 and C_2, respectively. In the modified concentration scheme, the initial value in system 2 is again zero ($C_2^{*0} = 0$), while the concentration at the boundary is $C_1^{*0} = C_1^0 - C_2^0$. We then apply Eqs. 17-9 and 17-12 to the modified concentrations. By adding C_2^0 to the result (Eq. 17-9), we transform the concentrations back to the original scale:

$$C_2(x,t) = C_2^0 + \left(C_1^0 - C_2^0\right) \operatorname{erfc}\left(\frac{x}{2(Dt)^{1/2}}\right) \quad \text{for } x \geq 0 \tag{17-13}$$

All the equations remain valid if the initial concentration, C_2^0, is larger than C_1^0. Figure 17.3*c* shows the case where C_1^0 is zero and remains zero for $t > 0$. Then, the modified concentration, C_1^*, as well as the integrated mass flux (Eq. 17-12) are negative. The latter means that the direction of the flux is reversed, that is, from system 2 to system 1.

Two-Sided Diffusion from a Boundary. Next, we consider the case of two-sided diffusion across a boundary. Again, systems 1 and 2 are placed in contact via a flat boundary at $x = 0$, but now the concentration in system 1 is not held constant. Transport on both sides of the boundary is by diffusion. In system 1, the initial concentration is "eroded away," while the concentration builds up in system 2 (Fig. 17.4). As before, we redefine the concentrations such that the initial concentration in system 2 is zero:

$$\begin{aligned} C_1^*(x,t) &= C_1(x,t) - C_2^0 \quad \text{and} \quad C_1^*(x,t=0) = C_1^0 - C_2^0 \equiv \Delta C \\ C_2^*(x,t) &= C_2(x,t) - C_2^0 \quad \text{and} \quad C_2^*(x,t=0) = 0 \end{aligned} \tag{17-14}$$

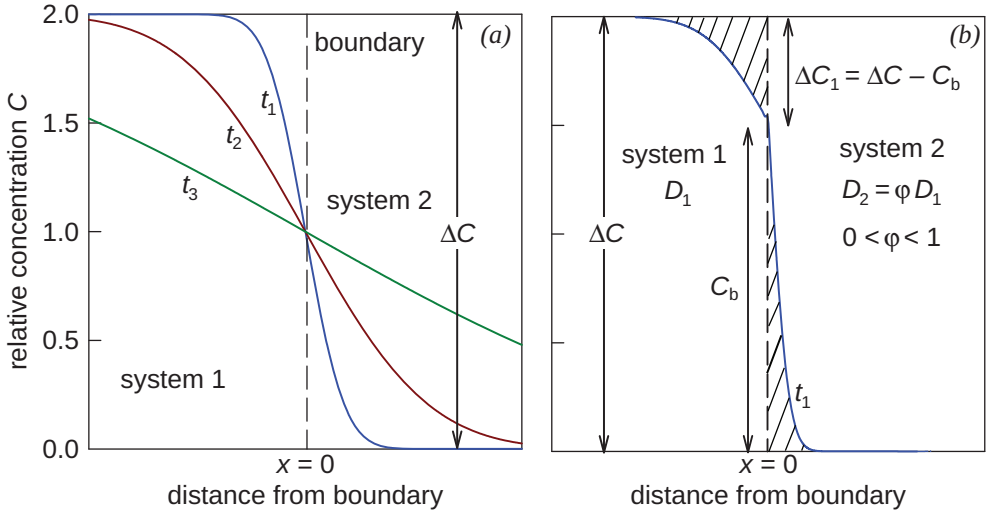

Figure 17.4 (*a*) Solution for the symmetric time-dependent diffusion equation (Fick's second law, Eq. 6-34*b*) at a two-sided wall boundary (Eq. 17-15). ΔC is the initial concentration difference between system 1 and 2 (see Eq. 17-14). Diffusivities in both systems are equal: $D_1 = D_2 = D$. The three consecutive times are related by $t_2 = 10\ t_1$, $t_3 = 100\ t_1$. (*b*) Two-sided wall boundary with different diffusion coefficients in system 1 and 2 ($D_2 = 0.1\ D_1$). Profile is drawn for time t_1 only. The hatched areas on both sides of the boundaries are equal. The slope of the concentration profile changes discontinuously at the boundary due to the abrupt change of the diffusivity.

ΔC is the initial concentration jump at the boundary, having either sign. We first give the solution to Fick's second law (Eq. 6-34*b*) for the special case that diffusivities on both sides of the boundary are equal ($D_1 = D_2 = D$; symmetric diffusion):

$$C^*(x,t) = \frac{\Delta C}{2}\,\mathrm{erfc}\left(\frac{x}{2(Dt)^{1/2}}\right) \quad \text{for } -\infty < x < \infty \quad \text{where} \quad \Delta C = C_1^0 - C_2^0 \tag{17-15}$$

Again, we find the complementary error function, erfc(y), with the same argument as in Eq. 17-9. This time, the solution applies to both sides of the interface: $x < 0$ for system 1 and $x > 0$ for system 2. The interface is located at $x = 0$, where C^* (0,t) remains constant with time at $\Delta C/2$. The solution is symmetric around $x = 0$ in the sense that the profile on one side of the boundary is the mirror image of the profile on the other side (Fig. 17.4*a*).

As in Eq. 17-11, we can define a "penetration distance." Now, a "loss penetration" exists on one side of the boundary that is compensated for by the corresponding "gain penetration" on the other side of the boundary. The penetration proceeds as $(Dt)^{1/2}$.

We can also ask how much of the compound has crossed the interface at time t. The loss from system 1 corresponds to the gain of system 2. By analogy to Eq. 17-12, the exchanged mass is given by:

$$\mathcal{M}^*(t) = \int_0^\infty C^*(x,t)\mathrm{d}x = \left(\frac{1}{\pi}\right)^{1/2}(Dt)^{1/2}\Delta C = 0.564\,(Dt)^{1/2}\Delta C \tag{17-16}$$

The integrated mass exchange is proportional to the initial concentration difference ΔC and to $(Dt)^{1/2}$.

If the diffusivities are different in the two systems (e.g., $D_1 > D_2$), the concentration profile becomes asymmetric, and the boundary value is no longer at $\Delta C/2$. Yet the loss and gain, represented by the marked area on either side of the boundary, remain equal (Fig. 17.4*b*). This property can be used in order to calculate the concentration at the boundary. In Problem 17.5, you are asked to prove that the boundary concentration $C_\mathrm{b} = C(x = 0)$ is at:

$$C_\mathrm{b} = \Delta C\frac{1}{1+\varphi} \quad \text{with} \quad \varphi = \sqrt{\frac{D_2}{D_1}} \tag{17-17}$$

Since the diffusivities, D_1 and D_2, are different, the penetration depth is different on both sides of the boundary. For $\varphi = 1$, $C_\mathrm{b} = \Delta C/2$, as in Eq. 17-15. If $D_2 \ll D_1$, $C_\mathrm{b} \to \Delta C$, and the boundary becomes a one-sided wall boundary with a well-mixed compartment 1 (Fig. 17.3).

To summarize, all the concentration profiles derived in this subsection (Eqs. 17-8, 17-9, 17-13, and 17-15) are solutions of the same partial differential equation (Eq. 6-34*b*), that is, of Fick's second law. The reason that they look different is solely

the result of the different initial and boundary conditions. In Chapter 18, these mathematical tools will be used to study mass exchange of chemicals across different kinds of boundaries. Although the underlying mathematics remains the same, the properties of the chemicals, like sorption to solids or partitioning between different media, will make it necessary to modify some of these equations in order to apply them to specific environmental situations.

17.2 Molecular Diffusion

The thermal motion of atoms and molecules through gaseous, liquid, solid, or mixed media leads to molecular diffusion. This section deals with molecular diffusion coefficients of organic substances in gases (particularly air) and in aqueous solutions. Diffusion in porous media (e.g., soils and sediments) will be discussed at the end of the section.

The Complex Nature of Molecular Diffusion Processes

Fick's first law (Eq. 6-31) states that the diffusive flux is linearly related to spatial concentration gradients. In fact, a closer inspection of molecular transport shows that the driving force for a diffusive flux is the gradient of the chemical potential rather than the concentration. Hence, the two gradients are proportional to one another, unless temperature and pressure vary with space.

Molecular diffusion deals with the relative motion of one kind of atom or molecule against a set of reference molecules. As explained in Section 6.3 (Thought Experiment in a Train), the reference system itself may move relative to some chosen coordinates. We called the motion of the reference system advection. However, if one looks very closely and wants to use crystal clear definitions, it turns out that there is more than one way to choose the reference system. It could be the center of volume, the center of mass, or even the center of moles (that is, the center of number of molecules). Each choice leads to a different separation between diffusion and advection, and that results in a different diffusion coefficient. The center of volume is conceptually the best choice, although not all experimental setups yield this kind of diffusion coefficient. For a better understanding of this subtle and somewhat confusing matter, we recommend Chapters 3 and 5 of the book by Cussler (2009) on diffusion.

Molecular diffusivity depends on both the diffusing chemical and the medium, such as water (w), air (a), or any other gas or liquid (pure or mixture) like N_2, octanol, or diesel fuel. Chemical handbooks usually list diffusivities as *diluted two-component* or *binary* coefficients, such as the diffusion of tetrachloroethene relative to a pure gas (e.g., molecular nitrogen) or relative to air (D_{ia}). Although air contains many substances, the fairly constant mixing ratio of the two major components of air, N_2 and O_2, acts like a uniform reference system.

Related to binary diffusion is the coefficient of *self-diffusion*. As an example, we take a binary system of benzene and cyclohexane with different mixing ratio. At one end

(pure benzene), we find the coefficient of *self-diffusion* of benzene, at the other end, the coefficient of self-diffusion of cyclohexane. Coefficients of self-diffusion are relevant, for instance, when we tag a small amount of benzene by radioactive carbon and look at how the tagged benzene is mixed into the untagged benzene.

The diffusion of a chemical may also be influenced by intermolecular interactions between the solute and solvent. The effect becomes relevant when the solute and solvent form an association that diffuses intact (e.g., by hydration). Furthermore, intermolecular interactions between solvent molecules may influence diffusivities. As experimentally shown by Wilke and Chang (1955) and Witherspoon and Bonoli (1969), diffusion coefficients in water are significantly larger than diffusion coefficients in unassociated (i.e., non-hydrogen bonding) liquids. This phenomenon has to do with groups of water molecules forming clusters such that the diffusion step length, λ (see Eq. 17-6), is longer; this is mathematically modeled using an "association parameter" in the Wilke-Chang equation (Wilke and Chang, 1955; see Eq. 17-26).

Here, we confine ourselves to discussing molecular diffusion coefficients of organic molecules in the standard environmental systems of air and water. The used dimension of diffusivity is L^2T^{-1} (Eq. 6-30); thus, the standard metric unit is $m^2\ s^{-1}$. However, in most handbooks, diffusion coefficients are given in $cm^2\ s^{-1}$ ($= 10^{-4}\ m^2\ s^{-1}$), the unit also adopted here.

Diffusion Coefficients in Air

Molecular diffusion coefficients in air can be found in the scientific literature for a great number of organic chemicals (e.g., survey compiled by Yaws, 2009). Even a very large set of data cannot include all known organic chemicals, and new organic chemicals are continuously designed by the chemical industry. Therefore, it is important to get an understanding how the structure of a diffusing molecule influences its diffusivity. We can approach this aim in two ways, by theoretical considerations or by statistical analysis of measured diffusion coefficients.

According to the model of random walk in three dimensions, the diffusion coefficient in air of compound i, D_{ia}, can be expressed as one-third of the product of the mean free path, λ_i, and the mean three-dimensional velocity, $\overline{u}_i$ (Eq. 17-6*b*). In the framework of the molecular theory of gases, $\overline{u}_i$ is (e.g., Cussler, 2009):

$$\overline{u}_i = \left(\frac{8RT}{\pi M_i}\right)^{1/2} \qquad (\text{cm s}^{-1}) \tag{17-18}$$

where R is the gas constant (8.31×10^7 g cm^2 K^{-1} s^{-2} mol^{-1}), T is the absolute temperature (K), and M_i is the chemical's molar mass (g mol^{-1}).

The mean free path, λ_i, of a molecule in air must be inversely related to its collision cross section, $\mathcal{A}_i$. Picturing diffusing molecules as spheres with radius, r_i, the collision

cross-section is proportional to r_i^2. In turn, r_i can be estimated from the molar volume, $\overline{V}_i$:

$$r_i = \left(\frac{3\overline{V}_i}{4\pi N_A} \right)^{1/3} \tag{17-19}$$

where $N_A = 6.02 \times 10^{23}$ mol^{-1} is Avogadro's number. By disregarding all constant factors, we expect λ_i to depend on molecular size as:

$$\lambda_i = \text{const}(\mathcal{A}_i)^{-1} = \text{const}\left(r_i^{-2}\right) = \text{const}(\overline{V}_i)^{-2/3} \tag{17-20}$$

Equations 17-18 and 17-20 provide the rationale behind attempts to find simple empirical relations between D_{ia} and either $\overline{V}_i$ or M_i. In Fig. 17.5, the D_{ia} values listed in Yaws (2009) are plotted against $\overline{V}_i$ and M_i, respectively, for about 200 chemicals on a double-logarithmic plot. The molar volumes were calculated by the scheme developed by Abraham and McGowan (1987) and presented in Box 7.2. The correlation with molar volume is quite good (see Fig. 17.5*a*):

$$D_{ia}(\text{cm}^2\,\text{s}^{-1}) = (1.52 \pm 0.07)\,\overline{V}^{-(0.67\pm0.01)}, \quad \overline{V} \text{ in } (\text{cm}^3\,\text{mol}^{-1}) \tag{17-21a}$$

This fitted correlation yields the exponent –2/3 as predicted by Eq. 17-20. Alternatively, D_{ia} also shows a clear inverse relation with molar mass, M_i, with an exponent that is very close to –1/2 (see Fig. 17.5*b*), as predicted by Eq. 17-18:

$$D_{ia}(\text{cm}^2\,\text{s}^{-1}) = (0.83 \pm 0.09)\,M_i^{-(0.51\pm0.02)}, \; M_i \text{ in } (\text{g}\,\text{mol}^{-1}) \tag{17-21b}$$

However, the variance in Eq. 17-21*b* is significantly larger than for the correlation with molar volume, which largely stems from assuming a constant molar density

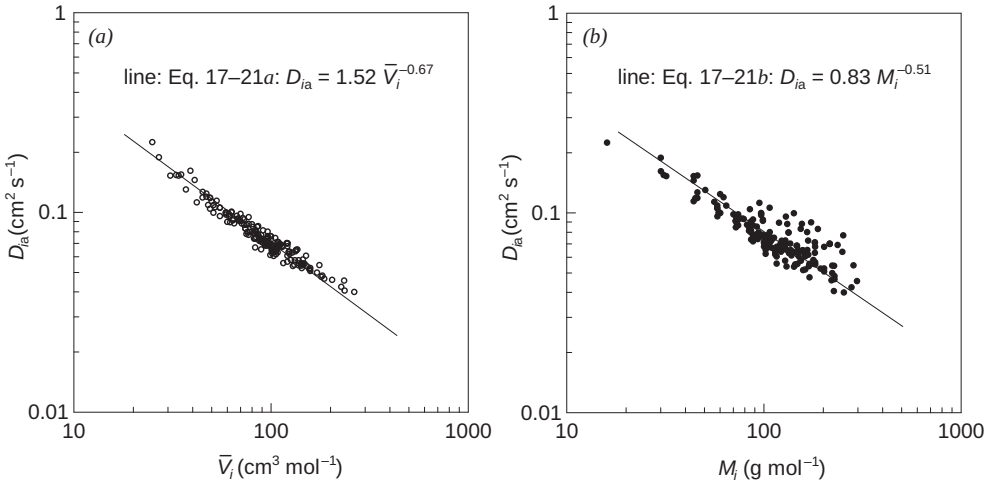

Figure 17.5 Molecular diffusion coefficients in air, D_{ia}, at 25°C for about 200 molecules plotted as a function of (*a*) their liquid molar volume, $\overline{V}_i$ (calculated by the method of Abraham and McGowan (1987), see Box 7.2) and (*b*) their molar mass, M_i. Data from Yaws (2009).

for all these substances in order to use M_i as a metric of their relative molecular sizes.

The simple relations given in Fig. 17.5 can serve as first estimates for D_{ia}. If data are missing, the correlations can also be used to estimate D_{ia} of a chemical from the known D_{ia} value of a reference chemical with similar molecular properties (particularly molar density):

$$\left(\frac{D_{ia}}{D_{ref\,a}}\right) = \left(\frac{\overline{V}_i}{\overline{V}_{ref}}\right)^{-2/3} \quad \text{or} \quad \left(\frac{D_{ia}}{D_{ref\,a}}\right) = \left(\frac{M_i}{M_{ref}}\right)^{-1/2} \tag{17-22}$$

Since molar volume is approximated by the element composition method by Abraham and McGowan (1987), all three approaches give identical D_{ia} values for structural isomers.

Fuller et al. (1966) proposed a semi-empirical relation that is based on the "$\overline{u}_i$ times λ_i" concept:

$$D_{ia} = 10^{-3}\frac{T^{1.75}[(1/M_{air}) + (1/M_i)]^{1/2}}{p\left[\overline{V}_{air}^{1/3} + \overline{V}_i^{1/3}\right]^2} \quad (\text{cm}^2\,\text{s}^{-1}) \tag{17-23}$$

where T is the absolute temperature (K), M_{air} is the average molar mass of air (28.97 g mol^{-1}), M_i is the chemicals molar mass (g mol^{-1}), p is the gas phase pressure (atm), $\overline{V}_{air}$ is the average molar volume of air (20.1 cm^3 mol^{-1}), and $\overline{V}_i$ is the chemical's molar volume (cm^3 mol^{-1}). Equation 17-23 is not dimensionally correct and is, thus, only valid if all the quantities are expressed in the units listed. This relation takes into account the fact that both types of molecules, the chemical i as well as the molecules of the surrounding medium "air", are moving. As one can show, the relevant mean molecular "composite velocity" follows from Eq. 17-18 by replacing $1/M_i$ by $(1/M_i + 1/M_{air})$. Regarding the mean free path, the critical distance for collision is not just r_i, but the sum of r_i and r_{air}, where both lengths are approximated by the cube roots of the corresponding molar volumes (Eq. 17-20).

Importantly, the expression also incorporates dependencies on the gas temperature ($T^{1.75}$) and pressure (p^{-1}). One part of the T-dependence comes from Eq. 17-18 ($T^{0.5}$), an additional factor (T/p) originates from the gas equation and expresses the gas volume (air) in which the chemical i is diffusing. Thus, up to the remaining $T^{0.25}$, we can at least qualitatively understand the structure of Fuller's approximation (Eq. 17-23).

As an illustration to compare the presented approaches, molecular diffusion coefficients in air are calculated for three chemicals compared to the measured value given by Yaws (2009) (Table 17.1). For the evaluation of Eq. 17-23, we calculate $\overline{V}_i$ from liquid density, as in Fuller et al. (1966), while for the correlation of Fig. 17.5*a* we use $\overline{V}_i$ from Abraham and McGowan (1987), i.e., the values used to derive Eq. 17-21*a*.

Table 17.1 Estimating Molecular Diffusion Coefficients in Air, D_{ia}, by Different Methods

	Trichloromethane $CHCl_3$	Benzene C_6H_6	*n*-Hexadecane $C_{16}H_{34}$
M_i (g mol^{-1})	119.4	78.1	226.4
$\rho_{i,\text{liquid}}$ (g cm^{-3})	1.49	0.876	0.77
$\overline{V}_i$(a) $= M_i / \rho_{i,\text{liquid}}$ (cm^3 mol^{-1})	80.1	89.1	294
$\overline{V}_i$(b) from Box 7.2 (cm^3 mol^{-1})	61.7	71.6	236
D_{ia} (cm^2 s^{-1}) (25°C, 1 atm) (deviation relative to measured)			
Measured (Yaws 2009)	0.0891	0.0935	0.0405
From Eq. 17-21*a* using $\overline{V}_i$ (b)	0.096 (+8%)	0.087 (–7%)	0.039 (–4%)
From Eq. 17-21*b* using M_i	0.072 (–19%)	0.090 (4%)	0.052 (+28%)
From Fuller et al. (Eq. 17-23) using $\overline{V}_i$ (a)	0.090 (+1%)	0.090 (–4%)	0.048 (+18%)

The best agreement between approximations and measurement is achieved for benzene, the chemical whose molar mass and volume lie in the middle of the substances used for the correlations Eqs. 17-21*a* and *b*. For the heavy chemical, *n*-hexadecane, the agreement between the different methods is less satisfactory. It is remarkable that the simple correlation between D_{ia} and $\overline{V}_i$ seems to be as good as the more refined method by Fuller et al. (Eq. 17-23). In contrast, the correlation between D_{ia} and M_i shows a distinct bias (underestimation for small molar mass, overestimation for large mass).

Diffusion Coefficients in Water

Yaws (2009) also surveyed molecular diffusion coefficients of organic solutes in water, D_{iw}. Diffusion coefficients in water are about 10^4 times smaller than those in air. Based on what we have learned from the random walk model, most of the difference between D_{ia} and D_{iw} can be attributed to the density ratio between water and air (about 10^3) that leads to a much smaller mean free path in water.

Again, it is important to analyze the factors that influence D_{iw}. As in air, it is plausible that D_{iw} depends on the diffusate's size. Using molar volume, $\overline{V}_i$, to characterize size, we see D_{iw} ranging from about 2×10^{-5} cm^2 s^{-1} for small molecules ($\overline{V}_i$ about 30 cm^3 mol^{-1}) to about 0.5×10^{-5} cm^2 s^{-1} for molecules with molar volume of 250 cm^3 mol^{-1} or more (Fig. 17.6*a*). Again, one can find a good empirical relation between molecular diffusivities in water and molecular volume as estimated by the method of Abraham and McGowan:

$$D_{iw}(\text{cm}^2\ \text{s}^{-1}) = (1.52 \pm 0.07) \times 10^{-4} \overline{V}^{-(0.64 \pm 0.01)}, \overline{V} \text{ in } (\text{cm}^3\ \text{mol}^{-1}) \quad (17\text{-}24a)$$

A similar relationship holds between molar mass, M_i, and D_{iw} (Fig. 17.6*b*):

$$D_{iw}(\text{cm}^2\ \text{s}^{-1}) = (7.0 \pm 0.08) \times 10^{-5}\ M_i^{-(0.45 \pm 0.02)},\ M_i \text{ in } (\text{g mol}^{-1}) \quad (17\text{-}24b)$$

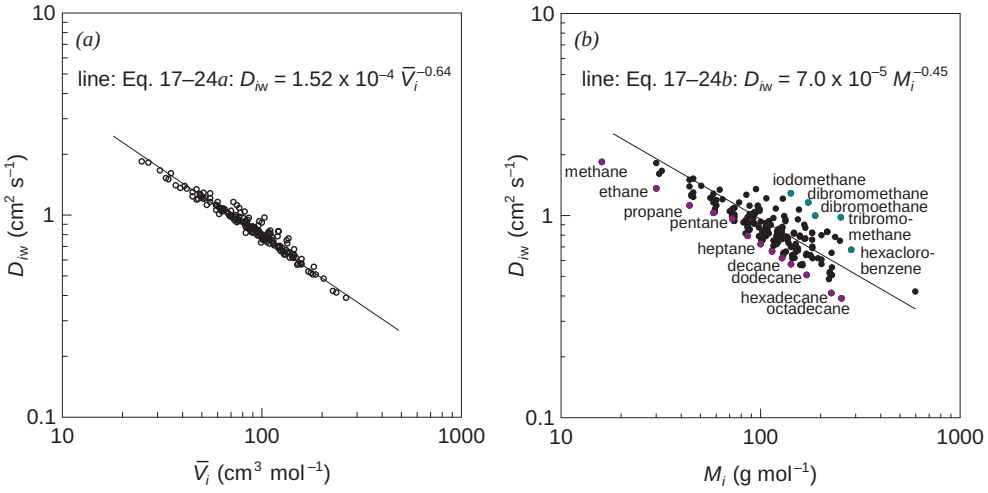

Figure 17.6 Molecular diffusion coefficients, D_{iw}, at 25°C of molecules in water plotted as a function of (*a*) their liquid molar volumes, $\overline{V}_i$ (calculated by the method of Abraham and McGowan (1987), see Box 7.2) and (*b*) their molar mass, M_i. In (*b*), halogenated compounds with above-average liquid densities and *n*-alkanes with below-average liquid densities are separately denoted. Data from Yaws (2009).

The fact that the relationship of M_i and D_{iw} in Fig. 17.6*b* shows significantly more variance than the one between $\overline{V}_i$ and D_{iw} in Fig. 17.6*a* means that the liquid density, $\rho_{iL} = M_i/\overline{V}_i$, of some of these chemicals significantly deviates from the mean (typically 1 g cm^{-3}). Halogenated compounds (see Fig. 17.6*b*) have liquid densities above 2 g mol^{-1}. Their molar mass overestimates their relative size. In turn, the *n*-alkanes (see Fig. 17.6*b*) have liquid densities near 0.7 g mol^{-1}. Molar mass underestimates their relative size. Instead, if diffusivity is related to molar volume, both types of compounds behave as most other substances (Fig. 17.6*a*).

The random walk model (Eq. 17-6) is somewhat less suitable for a liquid than for a gas. The close packing of the molecules inhibits their molecular motion. In water, molecules move less in a "go-hit-go" mode, but rather experience continuously varying intermolecular forces more analogous to viscous forces or drag. The drag is proportional to the viscosity of the fluid and the size (radius) of the molecule. The larger the drag, the smaller is the movement of the molecules. Thus, we expect that D_{iw} values will also depend inversely on the viscosity of the medium and the size (molar radius or volume) of the organic solute.

Based on this concept, Othmer and Thakar (1953) derived the following empirical expression with coefficients modified slightly by Hayduk and Laudie (1974):

$$D_{iw} = \frac{13.26 \times 10^{-5}}{\eta^{1.14}\overline{V}_i^{0.589}} \quad (\text{cm}^2\ \text{s}^{-1}) \tag{17-25}$$

where η is the solution viscosity in centipoise (10^{-2} g cm^{-1}s^{-1}) at the temperature of interest, and $\overline{V}_i$ is the molar volume of the chemical (cm^3 mol^{-1}). This equation is only valid if all quantities are given in the prescribed units. Since viscosity decreases by about a factor of two between 0°C and 30°C (Appendix B.3, Table B.3*a*), D_{iw} should increase by about the same factor over this temperature range.

Table 17.2 Estimating Molecular Diffusion Coefficients in Water, D_{iw}, by Different Methods

	Benzene C_6H_6	Trichloroethene C_2HCl_3	*n*-Hexadecane $C_{16}H_{34}$
M_i (g mol^{-1})	78.1	131.4	226.4
$\rho_{i,\text{liquid}}$ (g cm^{-3})	0.876	1.46	0.77
$\overline{V}_i$ (a) $= M_i / \rho_{i,\text{liquid}}$ (cm^3 mol^{-1})	89.1	90.0	294
$\overline{V}_i$ (b) from Box 7.2 (cm^3 mol^{-1})	71.6	71.5	236
D_{iw} (10^{-5} cm^2 s^{-1}) (25°C, 1 atm) (error relative to measured)			
measured (Yaws 2009)	1.159	0.993	0.413
From Eq. 17-24*a* using $\overline{V}_i$ (b)	0.98 (–15%)	0.98 (–1%)	0.46 (–11%)
From Eq. 17-24*b* using M_i	1.00 (–14%)	0.79 (–20%)	0.62 (+50%)
From Hayduk and Laudie (Eq. 17-26) using $\overline{V}_i$ (a)	1.07 (–8%)	1.06 (+7%)	0.53 (+28%)
From Wilke-Chang (Eq. 17-27*a*) using $\overline{V}_i$ (a)	1.14 (–2%)	1.13 (+14%)	0.56 (+36%)

Furthermore, the influence of the molecule's size is somewhat weaker than one sees for diffusion in gases (Eq. 17-22).

Let us now compare Eq. 17-25 with the empirical relation derived in Fig. 17.6*a* for D_{iw} at 25°C. With $\eta(H_2O, 25°C) = 0.890 \times 10^{-2}$ g cm^{-1}s^{-1}, Eq. 17-25 becomes:

$$D_{iw}(\text{cm}^2\,\text{s}^{-1}) = 1.514 \times 10^{-4}(\overline{V}_i)^{-0.589} \tag{17-26}$$

Comparing this equation to Eq. 17-24*a*, one sees that the agreement is very good, which is also seen when we calculate D_{iw} for specific compounds by the different methods and compare them to the measured values given by Yaws (2009) (Table 17.2).

As first shown by Wilke and Chang (1955) and later confirmed by Witherspoon and Bonoli (1969), the viscosity of the fluid is not the only influence of the fluid on molecular diffusion in a solute. Due to the especially strong association of hydrogen-bonding molecules in some liquids like water, D_{iw} is enhanced compared to diffusion in unassociated liquids. That is, since water molecules connect to each other so extensively via hydrogen bonding, they do not move as individuals but rather in "packs." To address this, Wilke and Chang (1955) proposed the following empirical equation:

$$D_{iw} = 7.4 \times 10^{-8} \frac{(\xi M_{\text{solvent}})^{0.5} T}{\eta(\overline{V}_i)^{0.6}} \quad (\text{cm}^2\,\text{s}^{-1}) \tag{17-27}$$

where x is the association parameter (1 for unassociated liquids like benzene and heptane, 1.9 in methanol, and 2.6 for water), and M_{solvent} is molar mass of solvent in g mol^{-1}. The units of the other variables are as in Eq. 17-25. Replacing the variables with the corresponding numerical values for water yields:

$$D_{iw}(\text{cm}^2\,\text{s}^{-1}) = 1.695 \times 10^{-4}(\overline{V}_i)^{-0.6} \tag{17-27a}$$

Looking at the results in Table 17.2, we see the best agreement between approximation and measurement is achieved with the exponential function given in Eq. 17-24*a*, not surprising given the good correlation found in Fig. 17.6*a*. Remember that, except for the approximation method using Eq. 17-24*b*, based on the correlation found in Fig. 17.6*b*, once water temperature is given, all other approximations are simple exponential functions of molar volume $\overline{V}_i$.

Molecular Diffusivities in Porous Media

So far, we have assumed that the movement of the molecules is not restricted by "impenetrable" materials like solids; that is, the diffusive volumes have been entirely filled with gaseous or liquid fluids in which diffusion occurs (e.g., air, water). This assumption does not hold in many solid-containing systems like soils, sediments, and activated carbon beds. Such combined fluid and solid systems are often called porous media, introduced in Section 5.4 with pores denoting gas and liquid filled spaces in the system. Here, we briefly discuss how molecular diffusivity is affected in porous systems.

Knudsen Effect (Gas Phase). The limited space effect is most prominent in gas-filled pores. If the typical pore diameter, d_p, is of the same order as the mean free path of molecule i, λ_i, then the molecule frequently collides with the pore walls and its diffusivity is reduced (see Eq. 17-6). This is called the *Knudsen Effect*, and the ratio λ_i/d_p is called the Knudsen number, Kn. If Kn is on the order of 1 or larger, λ in Eq. 17-6 has to be replaced by d_p. Since at atmospheric pressure, λ is typically on the order of 10^{-6} cm, the Knudsen effect becomes important for pore sizes smaller than 10^{-6} cm (i.e., 10 nm). In this case, diffusivity through the gas-filled spaces no longer depends on the inverse of pressure, p^{-1}, as in Eq. 17-23.

Renkin Effect (Liquid Phase). In liquids, the mean free path is typically of the order of 10^{-8} cm. Hence, the Knudsen effect is not important (i.e., diffusing molecules collide with solvent molecules long before they typically arrive at a pore wall). However, diffusion is affected by a different mechanism, the viscous drag associated with the diffusing molecule's attractions to the pore walls, known as the *Renkin effect* (Renkin, 1954), or constrictivity (e.g., Gaiselmann et al., 2014). In essence, the reduction of pore diffusivity in the liquid-filled pore space relative to diffusivity in the free liquid depends on the Renkin ratio, $q_R = d_i/d_p$, where d_i is the molecular diameter of the solute, and d_p is pore diameter. Various empirical and theoretical expressions that relate the relative reduction of pore diffusivity to the Renkin ratio (see, e.g., Renkin, 1954; Quinn et al., 1972). In essence, the Renkin effect sets in when d_p becomes smaller than about 10^3 d_i and suppresses diffusion completely when d_p approaches d_i. Diffusing molecules have a typical size of 10^{-8} to 10^{-7} cm (or 1 to 10 Å).

Porosity and Tortuosity. Knudsen and Renkin effects are only relevant for very small pores. In many cases, as in oceanic and lacustrine sediments, diffusive transport chiefly depends on porosity and tortuosity, two macroscopic porous media parameters. The volume fraction filled by gas or liquid is called porosity, ϕ (see Chapter 5, Box 5.4). As porosity decreases, the cross section available for transport is reduced.

Tortuosity, τ, is defined as the ratio of the mean path length connecting two arbitrary points to the length of the straight line between these points. Tortuosity increases the mean path length connecting two arbitrary points in space and, thus, reduces the concentration gradient along the path, the "driving force" in Fick's first law (Eq. 6-31). Boudreau (1996) compared tortuosity values measured in fine-grained sediments with various theoretical tortuosity-porosity relations. For porosities larger than 0.7, measured and calculated tortuosities are between 1 and 3. In water-saturated soils, tortuosity typically lies between 2 and 10 (Gao et al., 2014). For unsaturated soils, Hillel (1998) discusses different empirical expressions that relate tortuosity, τ, to total (air- and water-filled) porosity, ϕ, and to relative air content, $\theta_{g\,rel}$, defined by

$$\theta_{g\,rel} = \theta_g/\phi \tag{17-28}$$

where ϕ is the total (air- and water-filled) porosity, and θ_g is the volumetric gas content of the soil ($0 \leq \theta_g \leq \phi \leq 1$). All these expressions reflect the same effect; tortuosity becomes very large if $\theta_{g\,rel}$ and ϕ are small.

Bulk Diffusivity. Since molecular diffusivities in gases (e.g., in air) are orders of magnitude larger than those in liquids (e.g., water) and diffusivities in liquids are orders of magnitude larger than in the solid phase, the overall diffusive transport per total area, the so-called bulk diffusivity, is typically determined by transport in the least dense phase. This trend holds true unless the less dense phase occupies only a tiny fraction of the total volume or the partition coefficient governing the diffusate's presence in the two competing phases overcompensates for the enhanced diffusivity in one of the phases. For instance, in the unsaturated part of the soil, where all three phases co-exist (solids, water, and air), bulk diffusivity is primarily determined by diffusion through the gas-filled pores. In soils below the water table and in sediments, the role of the "diffusion carrier" is taken over by the liquid-filled (water-filled) pores. Only in solid rocks with virtually zero porosity does diffusion in solids become relevant. A quantitative framework for assessing the relative importance of diffusion in the gaseous and aqueous phase is given in Box 17.1.

Let us now analyze the influence of the physical structure of a porous medium, characterized by the two macroscopic parameters, porosity and tortuosity, on bulk diffusivity. We first analyze a chemical compound that does not undergo transfer processes between different phases such as sorption. The diffusive (gaseous or liquid) flux, $F_{i\text{pore}}$, within the pores for a chemical, i, can be written as:

$$F_{i\text{pore}} = -D_{i\text{pm}}\frac{\partial C_i}{\partial \xi} \qquad \left[\mathrm{ML_p^{-2}\,T^{-1}}\right] \tag{17-29}$$

where $D_{i\text{pm}}$ is diffusivity of species i in the porous medium [$\mathrm{L_p^2\,T^{-1}}$], taking into account the Knudsen or Renkin Effect, C_i is concentration in the pore space [$\mathrm{ML_p^{-3}}$], and ξ is distance along the pore [$\mathrm{L_p}$]. For clarity, we mark a difference between the spatial dimension of pore space [$\mathrm{L_p}$] and bulk space [$\mathrm{L_b}$]. Thus, porosity that otherwise would be nondimensional, has dimensions [$\mathrm{L_p^3\,L_b^{-3}}$].

In contrast, the diffusive flux per unit bulk area can be written as:

$$F_{i\text{bulk}} = -\phi D_{i\text{bulk}} \frac{\partial C_i}{\partial x} \left[\mathrm{ML_b^{-2}T^{-1}}\right] \tag{17-30}$$

where $D_{i\text{bulk}}$ is the diffusivity of species i per bulk area [$\mathrm{L_b^2\,T^{-1}}$], ϕ is porosity [$\mathrm{L_p^3 L_b^{-3}}$], and x is bulk distance [$\mathrm{L_b}$]. The factor ϕ on the right-hand side of Eq. (17-30) reflects the fact that the cross section available for transport is reduced due to the finite pore space.

In order to find a relation between $D_{i\text{pm}}$ and $D_{i\text{bulk}}$, we note that tortuosity, τ, both reduces the *in situ* concentration gradient along the real diffusion path and increases the real distance of transport relative to the bulk distance, x. The first effect is expressed mathematically by:

$$\frac{\partial C_i}{\partial \xi} = \frac{\partial C_i}{\partial x}\frac{\mathrm{d}x}{\mathrm{d}\xi} = \frac{1}{\tau}\frac{\partial C_i}{\partial x} \tag{17-31}$$

At the same time, the effect of the prolonged diffusion path is given by $F_{i\text{pore}} = \tau F_{i\text{bulk}}$. This two-fold effect is incorporated in the porous medium diffusivity $D_{i\text{pm}}$ by (see Boudreau, 1996):

$$D_{i\text{bulk}} = \frac{D_{i\text{pm}}}{\tau^2} \tag{17-32}$$

When we repeat the procedure outlined in Section 6.4 (Eqs. 6-33 and 6-34) to derive Fick's second law, we must take into account that the volume in which the concentration change is occurring due to the diffusive flux is reduced by porosity, ϕ, relative to the bulk volume. Thus, Eq. 6-34*b* carries an extra factor on the left-hand side:

$$\phi\frac{\partial C_i}{\partial t} = -\frac{\partial F_i}{\partial x} \tag{17-33}$$

Inserting Eq. 17-30 into Eq. 17-33 yields:

$$\phi\frac{\partial C_i}{\partial t} = \frac{\partial}{\partial x}(\phi D_{i\text{bulk}})\frac{\partial C_i}{\partial x} \tag{17-34}$$

If ϕ and $D_{i\text{bulk}}$ are constant along x, Eq. 17-34 becomes after division by ϕ:

$$\frac{\partial C_i}{\partial t} = D_{i\text{bulk}}\frac{\partial^2 C_i}{\partial x^2} \tag{17-35}$$

This is the same result as in Eq. 6-34*b* with the only exception that the homogeneous diffusion coefficient, D_i, is replaced by $D_{i\text{bulk}}$, which is usually smaller. Beside tortuosity (Eq. 17-30), the finite pore space may have a reducing influence as well (Knudsen and Renkin effect). In total, while porosity changes the form of Fick's first law, Fick's second law remains unchanged except for the influence on diffusivity.

Diffusion of Sorbing Chemicals in Porous Media: Effective Diffusivity

Until now, we have tacitly assumed that the diffusing compound does not interact chemically with the solid matrix of the porous media. However, in sediments and saturated soils the solid-to-fluid ratio, r_{sf}, is much larger than in open water. Thus, even for substances with medium or even small solid-water equilibrium distribution coefficients, K_{id}, the sorption of chemicals onto the surface of solids or into the solids may become important. In unsaturated soils, exchange between the gaseous and liquid phase may also be significant. In essence, the spatial migration by diffusion of a sorbing chemical may be several orders of magnitude smaller than diffusivity of a nonsorbing chemical, an effect called retardation (Eq. 12-24). The corresponding diffusion coefficient that enters the law by Einstein and Smoluchowski (Eq. 6-36) is called the effective diffusion coefficient, $D_{i\text{eff}}$. The mathematical theory is summarized in Box 17.1.

Box 17.1 Diffusive Transport of Sorbing Chemicals in Sediments and Saturated Soils: Effective Diffusivity

We consider a sorbing chemical i that diffuses in the pore space of a porous medium filled with water, assuming that sorption equilibrium between the solids and the fluid is attained everywhere and at all times. A distinction is made between the "bulk" dimension (L_b) and the pore space dimension. Since here it is assumed that the pores are completely filled with water, we call the corresponding dimension L_w. We also distinguish between the dimension of solid mass of the medium (M_s) and of chemical i (M_i).

C_{it}	Total (fluid and sorbed) concentration per bulk porous medium volume $[M_i L_b^{-3}]$
C_{id}	Concentration in water per bulk volume $[M_i L_b^{-3}]$
$f_{iw} = C_{id}/C_{it}$	Fraction of compound in water
$C_{iw} = C_{id}/\phi$	Concentration in water per pore volume $[M_i L_w^{-3}]$
ϕ	Porosity $[L_w^3 L_b^{-3}]$
r_{sw}	Solid-to-water phase ratio, as in Eq. 12-22 $[M_s L_w^{-3}]$
$K_{id} = C_{is}/C_{iw}$	Solid–water distribution coefficient, as in Eq. 12-8 $[M_s^{-1} L_w^3]$
$D_{i\ \text{bulk}}$	Bulk diffusion coefficient in porous medium (Eq. 17-32) $[L_b^2 T^{-1}]$
C_{is}	Concentration on solids $[M_i M_s^{-1}]$

Only diffusion of the chemical i through fluid-filled pore space is assumed to be important (i.e, no diffusion through or on surfaces of solids). According to Fick's first law (Eq. 17-30), the flux per bulk area can be written as:

$$F_{i\text{bulk}} = -\phi D_{i\text{bulk}} \frac{\partial C_{iw}}{\partial x} \qquad \left[ML_b^{-2}T^{-1}\right] \tag{1}$$

While the flux is independent of sorption of the chemical *i* on the solid phase, the movement of the concentration front through the porous medium is not. By applying Gauss' theorem (Eq. 6-33) in one dimension to the total concentration per bulk volume, C_{it}, we get:

$$\frac{\partial C_{it}}{\partial t} = -\frac{\partial F_{ibulk}}{\partial x} = \frac{\partial}{\partial x}\left(\phi D_{ibulk}\frac{\partial C_{iw}}{\partial x}\right) \tag{2}$$

If ϕ, f_{iw} and D_{ibulk} are constant along the *x*-axis, on the right-hand side of Eq. 2 we can replace the spatial gradient of C_{iw} by the gradient of C_{it}:

$$\frac{\partial C_{iw}}{\partial x} = \frac{f_{iw}}{\phi}\frac{\partial C_{it}}{\partial x} \tag{3}$$

Inserting Eq. 3 into Eq. 2 yields Fick's second law modified for a sorbing chemical:

$$\frac{\partial C_{it}}{\partial t} = f_{iw}\, D_{ibulk}\, \frac{\partial^2 C_{it}}{\partial x^2} = D_{ieff}\frac{\partial^2 C_{it}}{\partial x^2} \tag{4}$$

where the effective diffusivity of the total concentration (C_{it}) of a sorbing chemical in a porous medium, D_{ieff}, is:

$$D_{ieff} = f_{iw}\, D_{ibulk} \quad \text{with} \quad f_{iw} = \frac{1}{1 + r_{sw}\, K_{id}} \tag{5}$$

D_{ibulk} is the bulk diffusion coefficient of the chemical in the porous medium as defined in Eq. 17-32. The fraction of the chemical in the pore space, f_{iw}, is the reciprocal of the retardation factor, R_{fi}, defined in Eq. 12-24.

17.3 Other Random Transport Processes in the Environment

Smoke from oil burns at the site of the Deepwater Horizon oil spill in 2010. Photo: Stumberg (2010).

The concept of diffusion as a process of random transport is not restricted to the case of molecular diffusion in liquids and gases. In fact, diffusion is such a powerful model for the description of transport that it can be applied to processes which extend over more than 20 orders of magnitude. On the very slow side, it can be applied to the migration of molecules in solids, especially useful for movements of atoms and molecules in minerals that, although being rather slow, become effective over geological time scales. At temperatures of several hundred degrees Celsius, as they prevail in the earth's mantle, diffusivities of atoms in minerals (e.g., in feldspar) are of the order 10^{-6} to 10^{-3} cm^2 s^{-1} (Lerman, 1979). Diffusion in solids is usually highly anisotropic, i.e., it depends on the direction relative to the orientation of the crystal lattice. On the fast side, the concept of diffusion can also be applied to macroscopic transport, called *turbulent diffusion*. Turbulent diffusion is not based on thermal molecular motions, but on the mostly irregular (random) pattern of currents in water and air.

Turbulent Diffusion

The flow of fluids (e.g., water and air) is usually turbulent, rather than laminar. Laminar flow, in contrast to turbulent flow, is defined by a set of well-defined, distinct streamlines along which fluid elements flow. Turbulence evolves if the inertial forces, that is, the forces that act against changes in the direction of the flow at boundaries or at objects around which the flow occurs, override the viscous forces, the internal friction that keeps the flow smooth. The Reynolds number, Re, a nondimensional quantity, is a measure for the ratio of these forces, inertial versus viscous, defined by:

$$\mathrm{Re} = \frac{\text{inertia}}{\text{viscosity}} = \frac{d\,\mathrm{v}}{\eta_f/\rho_f} \tag{17-36}$$

where d is the spatial dimension of the flow system or object around which the flow occurs (m), v is the typical flow velocity (m s^{-1}), η_f is the dynamic viscosity of the fluid (kg $m^{-1}s^{-1}$), and ρ_f is the density of the fluid (kg m^{-3}).

For laminar flow, Re has to be smaller than a critical value of about 0.1. As an example, we take $v = 10^{-4}$ m s^{-1}, $(\eta_f/\rho_f) = 10^{-6}$ m^2 s^{-1} (corresponding to a water temperature of 20°C) and ask how large d can be to keep Re below 0.1. We get $d < \mathrm{Re}\,(\eta_f/\rho_f)/v = 10^{-3}$ m. Thus, only in the submillimeter pore space of sediments or aquifers would the flow field be purely laminar; flow would certainly not be laminar in an open water body such as a lake or the ocean, where length scales are much greater than millimeters.

Turbulent flow means that, superimposed on a large-scale flow field (e.g., the Gulf Stream), we find random velocity components along the flow (longitudinal turbulence) as well as perpendicular to the flow (transverse turbulence). The effect of the turbulent velocity component on the transport of a dissolved substance can be described by an expression which has the same form as Fick's first law (Eq. 6-31), where the molecular diffusion coefficient is replaced by the so-called turbulent or eddy diffusion coefficient, E [L^2T^{-1}]. For instance, for transport along the x-axis:

$$F_x = -E_x \frac{dC}{dx} \qquad [ML^{-2}T^{-1}] \tag{17-37}$$

and similarly for the other directional components. As in Eq. 17-6, we can visualize E_x to result from the product of a typical velocity (the turbulent velocity v_{turb}) and a typical mean free path (λ_{turb}).

Turbulent diffusion coefficients in natural systems (e.g., lakes, oceans, or atmosphere), are much larger than molecular coefficients (Table 17.3). Furthermore, turbulent diffusion is usually anisotropic (i.e., larger in the horizontal than the vertical direction) because, firstly, the extension of natural systems in the horizontal is usally larger than in the vertical. Thus, the structures of turbulence, often called eddies, that determine the mean free paths of random motion, λ_{turb}, often look like pancakes; that is, they extend along the horizontal axes but cannot grow along the vertical axis. Secondly, the atmosphere, oceans, and lakes are often density stratified, that

Table 17.3 Typical Molecular and Turbulent Diffusivities in the Environment

System	Diffusivity ($cm^2\ s^{-1}$) [a]
Molecular	
In water	$10^{-6} – 10^{-5}$
In air	10^{-1}
Turbulent in Ocean	
Vertical, mixed layer [b]	$0.1 – 10^4$
Vertical, thermocline and deep sea [b]	1 – 10
Horizontal [c]	$10^2 – 10^8$
Turbulent in Lakes	
Vertical mixed layer [b]	$0.1 – 10^4$
Vertical, thermocline and deep water	$10^{-3} – 10^{-1}$
Horizontal [c]	$10^1 – 10^7$
Turbulent in Atmosphere	
Vertical	$10^4 – 10^5$
Note: Horizontal transport mainly by advection (wind)	
Mixing in Rivers [d]	
Turbulent vertical	1 – 10
Turbulent lateral	$10 – 10^3$
Longitudinal by dispersion	$10^5 – 10^6$

[a] $1\ cm^2\ s^{-1} = 8.64\ m^2\ d^{-1}$.
[b] Data from Gargett (1984).
[c] Horizontal diffusivity is scale dependent (Okubo, 1971).
[d] Data from e.g., Fischer et al. (1979); Rutherford (1994).

is, the density changes along the vertical axis such that lighter fluids lie on top of heavier ones. As a consequence, gravitational forces keep the fluid parcels from moving too far vertically from the depth where they are neutrally buoyant. This compresses the eddies even further in the vertical direction. In a classic paper, Gargett (1984) studied the relationship between the strength of the vertical density gradient, usually expressed by the so-called Brunt-Väisälä or stability frequency, and vertical diffusivity in the ocean. Examples for such relations in lakes can be found in Imboden and Wüest (1995).

Diffusion Length Scales

Although extremely convenient, the description of turbulent diffusion by a Fickian type of expression (Eq. 17-37), has its limitations since the separation of a natural flow field into advection ("directed" transport) and diffusion is not unique but depends on the spatial scale. Imagine the effect of a natural current field on the distance d_{AB} between two objects, A and B. The mathematical form of the gradient-flux model used to describe turbulent diffusion does not take into account the fact that the turbulent diffusivity, E_x, is scale dependent. As long as d_{AB} is small, only the small eddies with size on the order of d_{AB} or smaller move A and B apart; that is, increase the distance d_{AB}. In contrast, the larger eddies move the two objects together in the same direction

like advective transport. The larger the d_{AB}, the larger the eddies that act on A and B as random transport or diffusion.

If we interpret the growing distance, d_{AB}, in terms of the Einstein-Smoluchowski law (Eq. 6-36) and calculate the "apparent" diffusivity, E_z, that explains the observed growth of d_{AB} with time, we find that E_z gets larger, the larger d_{AB} becomes. In other words, as a consequence of describing the effect of turbulence by the local concentration gradient (as done in Fick's law, Eq. 17-37), in a particular turbulent environment, smaller structures "experience" a smaller apparent diffusivity than larger ones. It also means that a spatial structure, as exemplified by d_{AB}, does not simply grow as the square root of ellapsed time, $t^{1/2}$, but rather growth is more like advection, linearly with time. In a seminal paper, Okubo (1971) related the apparent horizontal diffusivity to horizontal size ("Okubo diagram"). Since then, similar effects were found in other natural systems, e.g., in lakes (Imboden and Wüest, 1995).

Measurement of Vertical Turbulent Diffusivity

We now highlight another important difference between molecular diffusion and turbulent diffusion. Whereas the former is a characteristic property of the diffusing *chemical* that can be looked up, the latter is an individual, time-dependent property of the *system* (e.g., atmopshere, lake, or ocean), and not of the chemical. Although we can give typical sizes of turbulent diffusivity in different systems (Table 17.3), we could not look up specific values in a handbook. Therefore, methods are needed to determine turbulent diffusivity in a particular system.

A discussion of the different methods to determine turbulent difffusivity developed in the last 50 years goes beyond the scope of this book. Originally, the change of temperature, chemical concentrations, and radioactive isotopes (whether natural like radon-222, or man-made like tritium) were used to indirectly estimate turbulent transport. The temperature method is explained in Imboden et al. (1979). Broecker (1965) introduced the use of radiactive tracers for the measurements of diffusivity in the ocean. Imboden and Emerson (1978) used the same method for vertical diffusivity in lakes. A summary of other methods based on natural or man-made tracers can be found in Imboden and Wüest (1995). An example is given in Box 17.2 and Fig. 17.7.

Box 17.2 Calculating Vertical Turbulent Diffusivity from Radon Diffusion in Lakes and Oceans

The one-dimensional vertical diffusion-reaction equation of radon activity, A_{Rn}, is (Eq. 6.38, with v = 0):

$$\frac{\partial A_{Rn}}{\partial t} = E_z \frac{\partial^2 A_{Rn}}{\partial h^2} - \lambda_{Rn} A_{Rn} + \lambda_{Rn} A_{Ra} \qquad (1)$$

where

$\lambda_{Rn} = 0.181\ d^{-1}$ is the decay constant of radon-222,

E_z is vertical turbulent diffusivity ($m^2\ d^{-1}$), constant with depth,

h is vertical distance from sediment surface,

A_{Rn} is "radioactivity" of radon-222 (dpm L^{-1}), and

A_{Ra} is "radioactivity" of radium-226 (dpm L^{-1}).

"Radioactivity" of a radioactive isotope, rather than concentration, measures the number of decays per unit time and volume (dpm m^{-3} = decay per minute per m^3). When such "radioactivity" units are used, the *in situ* production of radon-222 from the decay of its precurser isotope radium-226 (last term on the right-hand side of Eq. 1) appears with the decay constant of radon-222 (rather than the one of radium-226) in the transport-reaction equation.

Replacing A_{Rn} by excess radon activity, $A_{Rn}^{exc} = A_{Rn} - A_{Ra}$, transforms Eq. 1 into:

$$\frac{\partial A_{Rn}^{exc}}{\partial t} = E_z \frac{\partial^2 A_{Rn}^{exc}}{\partial h^2} - \lambda_{Rn} A_{Rn}^{exc} \tag{2}$$

At steady state (i.e., $\partial A_{Rn}^{exc}/\partial t = 0$), the solution of Eq. 2 is:

$$A_{Rn}^{exc}(h) = A_{Rn}^{exc}(h=0) \exp\left[-\left(\frac{\lambda_{Rn}}{E_z}\right)^{1/2} h\right] \tag{3}$$

A plot of $\ln\{A_{Rn}^{exc}(h)\}$ versus height above sediments, h, should yield a straight line with slope $-(\lambda_{Rn}/E_z)^{1/2}$. Since λ_{Rn} is known, Ez can be determined from the slope (see Fig. 17.7).

With the development of high-resolution, fast sensors for temperature and current velocity, it became possible to measure turbulence directly. In fact, turbulent transport results from the covariance of the current velocity fluctuations with the fluctuation of concentration or temperature. Methods have been developed to determine turbulent diffusivity from the measurement of temperature microstructure (Osborn, 1980). A recent overview of how the method has developed can be found in Kawaguchi et al. (2014). These measurements yield instantaneous and local values for E_z.

Dispersion

As mentioned in Chapter 5 when discussion mixing in rivers (Section 5.3), in a flow field (river or aquifer), an additional process of random transport exists called dispersion. Dispersion results from the fact that the velocities in adjacent streamlines are different. For instance, in a river, the current velocities in the middle of the river are usually larger than on the sides. Due to lateral turbulence, water parcels randomly switch between different longitudinal streamlines. Thus, water parcels that spend more time in fast streamlines than in slow ones travel faster along the flow field and *vice versa*. Therefore, a concentration cloud originating, for instance, from a chemical accidentally dumped into a river within a short time period, is transformed into an elongated cloud while it travels downstream.

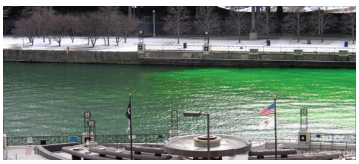

Diffusion of a chemical in a river. Photo: Knowledge Seeker (2005).

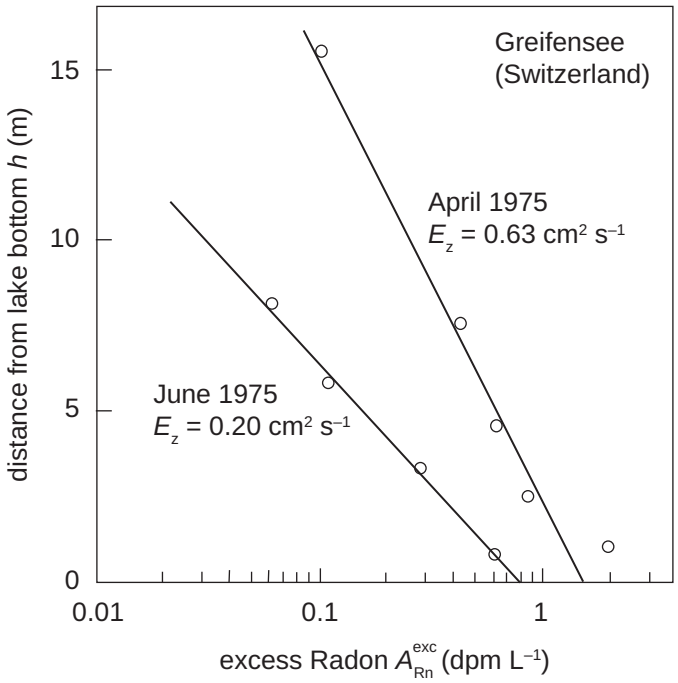

Figure 17.7 Vertical profiles of dissolved excess radon-222 activity (i.e., the radon-222 activity exceeding the activity of its parent nucleus radium-226 in units "decay per minute per liter" (dpm L^{-1}) in the bottom waters of Greifensee, Switzerland used to compute vertical turbulent diffusivity, E_z. Data from Imboden and Emerson (1978).

Fick's laws (Eq. 6-31 and 6-34*b*) can also be applied to dispersion. For a conservative substance (no *in situ* production or reaction), the one-dimensional advection-diffusion equation along the direction of flow, x, is reduced to the last two terms of Eq. 6.38 (J, $k = 0$):

$$\frac{\partial C}{\partial t} = \left(\frac{\partial C}{\partial t}\right)_{adv} + \left(\frac{\partial C}{\partial t}\right)_{disp} = -v_x \frac{\partial C}{\partial x} + E_{dis}\frac{\partial^2 C}{\partial x^2} \qquad (17\text{-}38)$$

where E_{dis} [L^2T^{-1}] is the longitudinal dispersion coefficient. The time-dependent solution of Eq. 17-38 is similar to Eq. 17-8, except for the fact that the maximum of the normal distribution moves with velocity, v, along the x-axis. This is reflected in the extra term ($-v_x t$) in the numerator of the exponential function:

$$C(x,t) = \frac{\mathcal{M}^*}{2(\pi E_{dis} t)^{1/2}} \exp\left(-\frac{(x - v_x t)^2}{4E_{dis} t}\right) \quad [ML^{-3}] \qquad (17\text{-}39)$$

where $\mathcal{M}^*$ is the mass of chemical per cross section perpendicular to the flow, v_x is the flow velocity in the downstream direction, and E_{dis} is the coefficient of dispersion. E_{dis} depends on the flow velocity, cross section of the river bed, and turbulence intensity.

17.4 Questions and Problems

Special note: Problem solutions are available on the book's website. Solutions to problems marked with an asterisk are available for everyone. Unmarked problems have solutions only available to teachers, practitioners, and others with special permission.

Questions

Q 17.1

Explain the difference between the coefficients, $p(n,m)$, and the function $p_n(m)$ defined in Eq. 17-2.

Q 17.2

By which mathematical/physical principle are the coefficients of the binominal distribution, $p(n,m)$, and Fickian diffusion related?

Q 17.3

Explain the relationship between Fick's first and second law? A general mathematical theorem explains it, which one? *Hint*: Chapter 6 may help.

Q 17.4

Prove the symmetry relations of the error functions given in Appendix A.2, Eq. 3.

Q 17.5

Explain the difference between the one-sided and symmetric diffusion at a wall boundary and why their solutions are nearly identical, except for a factor of 1/2.

Q 17.6

How would Eq. 17-10 be modified if instead of the half-concentration penetration distance one would define penetration distance by 10% of the original value at the boundary?

Q 17.7

What makes the definition of molecular diffusion coefficients in a NAPL (non-aqueous phase liquid) consisting of chemicals with very different molar mass vague?

Q 17.8

Explain the semi-empirical relation of Fuller et al. (1966) for molecular diffusivity in air (Eq. 17-23). How is this expression related to the molecular theory of gas?

Q 17.9

D_{iw} is well correlated with $\overline{V}_i$. Why then is it not really surprising that D_{iw} also correlates with molar mass M_i, although not as perfectly?

Q 17.10

What makes diffusion through a porous medium different from diffusion in open space? How do these factors differ between diffusion in gas (air) and in liquid (water) and why?

Q 17.11

Explain in words why at steady state ($\partial C_{it} / \partial t = 0$) the flux of a sorbing chemical in a porous medium is equal to the flux of a non-sorbing chemical (except for possible differences of their "normal" molecular diffusivities). What is really different for the two chemicals (sorbing *vs.* non-sorbing)?

Q 17.12

Why is turbulent diffusion in oceans and lakes usually anisotropic? Explain the term *anisotropy* both in mathematical and colloquial language. Give two reasons why turbulence in the vertical direction is special.

Q 17.13

Is it possible that advective transport of two solutes can simultaneously occur in opposite directions? What about diffusive transport?

Q 17.14

Where does *molecular* diffusion (in air or water) actually play a role in the environment? Give reasons why it is not relevant in systems or at specific places that you exclude in your answer.

Q 17.15

Why is turbulent diffusion scale-dependent, and what are the consequences?

Q 17.16

Explain, to a layperson, why the short half-life of radon-222 of about 4 days allows interpreting radon measurements as indicating steady-state conditions.

Problems

P 17.1 *Binominal Coefficients and Random Walk*

(a) Calculate the binominal coefficients $p(n,m)$ for $n = 8$, $m = 0, \pm 2, \ldots$ and complete Fig. 17.1 to 8 time steps. Compare the coefficients with the corresponding normal distribution function.

P 17.2 *First and Second Derivatives*

Draw the curves, $C(x)$, with the following properties: (a) $C' = 0$; (b) $C' \neq 0$, $C'' = 0$; (c) all combinations of $\pm C' > 0, \pm C'' > 0$; (d) $C' = 0$, $C'' = 0$, $C''' \neq 0$. Notation: $C' = \partial C/\partial x$, $C'' = \partial C^2/\partial x^2$, $C''' = \partial C^3/\partial x^3$.

P 17.3 *Non-constant Diffusivity*

Calculate flux F and concentration change $\partial C/\partial t$ for the one-dimensional concentration distribution $C(x) = a + bx$, if diffusivity increases along x: $D(x) = D_0 + gx$. The parameters, *a, b, g*, and D_0 are constant and positive.

Note: Such situations are found, for instance, in the vertical direction in the ocean where diffusivity occurs not by molecular motion but by turbulence. Turbulence intensity usually varies with depth.

P 17.4 *Decrease of Chloroform Concentration by Diffusion*

Molecular diffusion coefficient of chloroform in water: D_{iw} ($CHCl_3$) $= 5.5 \times 10^{-6}$ cm^2 s^{-1}

In order to illustrate the slowness of molecular diffusion, a colleague claims that one could place a droplet of water containing just 100 µg of chloroform into the middle of a stagnant water-filled pipe (diameter 4 cm), and that it would take at least one month until the concentration would not exceed a concentration of 1 mg L^{-1} anywhere in the pipe. How long does it really take?

Hint: Assume that the initial distribution is "point-like" (Eq. 17-7) and then use Eq. 17-8. Also, assume that the pipe is long enough so that its ends can be disregarded.

P 17.5 *Two-sided Diffusion at a Wall Boundary with Different Diffusivities*

Modify the formalism developed in Eqs. 17-14 to 17-16 for the case that the diffusivity in system 2 is smaller than in system 1. Prove Eq. 17-17.

P 17.6 *Temperature and Pressure Dependence of the Molecular Diffusion Coefficient in Air*

Estimate the molecular diffusion coefficient of tetrachloroethene in air, D_{ia}, at temperature $T = -10$°C and pressure $p = 0.5$ bar. Yaws (2009) gives D_{ia} at $T = 25$°C, $p = 1$ bar as 8.00×10^{-2} cm^2 s^{-1}.

P 17.7 *Molecular Diffusion Coefficient of a PCB Congener in Water,* D_{iw}

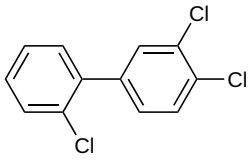

2',3,4-trichlorobiphenyl

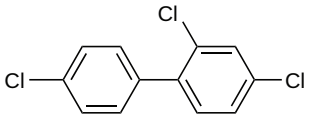

2,4,4'-trichlorobiphenyl

(a) You are in desperate need for the molecular diffusion coefficient of 2′,3,4-trichlorobiphenyl (TCBP) in water, D_{iw}, at 25°C but you cannot find any value in the literature. You are aware of several approximations. To make sure that they give reliable results, you try three of them.

(b) As you know the physicochemical properties of the various PCB congeners can be very different. Imagine you had to estimate D_{iw} for 2,4,4′-trichlorobiphenyl instead. Do the estimated values differ? What is the problem?

(c) Estimate the relative change of D_{iw} (TCBP) if the water temperature drops from 25°C to 0°C.

Dynamic viscosity of water

T (°C)	η (kg m^{-1}s^{-1})
0	1.79×10^{-3}
5	1.52
10	1.31
15	1.14
20	1.00
25	0.89

P 17.8 *Trifluoroacetic Acid in a Pond*

Trifluoroacetic acid is an atmospheric transformation product of freon substitutes. It enters surface waters by precipitation where it dissociates into its ionic form trifluoroacetate and then remains virtually inert. We want to estimate how much of the trifluoroacetate (TFA) would diffuse into the pore space of a small pond (volume V, area A) within one year.

CF_3–COOH ⇌ CF_3–COO^- + H^+
trifluoroacetic acid — trifluoroacetate

Pond characteristics

$V = 5 \times 10^4$ m^3
$A = 2 \times 10^4$ m^2
no through-flow

Help: For simplicity, assume that at a given time $t = 0$ the TFA concentration suddenly increases to some value, say $C_0 = 1$ μg L^{-1}. Consider the diffusion of TFA into the sediment by first assuming that the lake concentration C_0 remains constant. Calculate the fraction of TFA found in the sediment pores, $\mathcal{M}_{sed}/\mathcal{M}_0$, where $\mathcal{M}_0 = VC_0$. If this fraction is not too large, your assumption ($C_0 \sim$ const.) is justified. Use an effective molecular diffusivity of TFA in the sediment of $D_{i\text{eff}} = 10^{-5}$ cm^2 s^{-1}. Remember that sediments mostly consist of water.

P 17.9 *Evaluating the Effectiveness of a Polyethylene Membrane for Retaining Organic Pollutants in Relatively Dilute Wastewater*

You have been asked to comment on the likely effectiveness of a proposed 1 mm thick linear low density polyethylene (LLDPE) plastic sheet for retaining benzene present at ppm levels in wastewater. To be considered effective, the plastic sheet must retain the benzene for at least 20 years. Fortunately, you are aware of the study by Aminabhavi and Naik (1998). In that work, the investigators deduced the molecular diffusivities of several alkanes in plastics including LLDPE. Plotting their data as a function of chemical size (here, molar volumes), they found the following regression equation:

$$\log D_{i\text{LLDPE}} = -3.5 \log \overline{V}_i + 0.63$$

where diffusivity in LLDPE, $D_{i\text{LLDPE}}$, is in cm^2 s^{-1} and molar volume $\overline{V}_i$ in cm^3 mol^{-1}. The molar volume of benzene is $\overline{V}_i$ (benzene) = 89 cm^3 mol^{-1}. [Not surprisingly, diffusivities in the LLDPE are much less than corresponding diffusivities in water (e.g., $D_{hexane\ \text{LLDPE}} = 1.27 \times 10^{-7}$ cm^2 s^{-1} vs. $D_{hexane\ \text{water}} = 0.80 \times 10^{-5}$ cm^2 s^{-1}).]

If you define chemical breakthrough as the time it takes for the half-concentrations distance to become larger than the thickness of the plastic membrane, will a 1 mm thick LLDPE sheet be effective at retaining benzene for 20 years?

P 17.10* *Interpreting Stratigraphic Profiles of Polychlorinated Naphthalenes in Lake Sediments*

Gevao et al. (2000) reported the presence of polychlorinated naphthalenes (PCNs) in a lake sediment core taken in northwest England (see table). Like PCBs, these compounds were used by the electric industry as dielectric fluids in transformers and capacitors. You are interested in the question of when PCNs were first released in the area near the lake. Assume the lake sediments are always at 10°C, have 90% porosity, and their solids consist of 5% organic carbon.

Assuming a large pulse input in 1960 (i.e., causing a maximum concentration to appear in the 24-25 cm layer), is it reasonable to explain the observed concentrations in the 34-35 and 39-40 cm sections as due to diffusion from above?

M_i(PCNs) = 300.5 g mol^{-1}
log K_{iow} = 6.2 (average value)
ρ_s = 2.6 g cm$_s^{-3}$

Hint: Test the validity of the hypothesis that all the PCNs have entered the sediments in 1960 and that the PCN concentrations measured in older sediment layers can be explained by calculating diffusive displacement of PCN from the 1960-layer. Take into account the interaction of PCNs with the sediment matrix by calculating effective diffusivity.

PCN Concentration Profile

Depth (cm)	Year of deposition	PCN Concentration (ng kg^{-1} dry weight)
0-1	2000	1800
4-5	1992	4300
9-10	1984	4900
14-15	1976	6200
19-20	1968	12000
24-25	1960	18000
29-30	1952	8000
34-35	1944	120
39-40	1936	120
44-45	1928	0.0
49-50	1920	0.0

P 17.11 *Daydreams during Environmental Organic Chemistry Lectures*

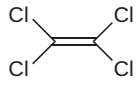

tetrachloroethene

You are an excellent student taking a very exciting subject, Environmental Organic Chemistry. Arriving at the lecture hall early, you take up a seat at the very front of the room. The lecture begins after all the students have taken their seats, and except for the wild gestures of your lecturer, the air in the room appears very still. Suddenly, an attractive individual enters the back of the room and takes a seat there about 10 meters away from you. After only about 1 minute, you notice a pleasant odor, presumably associated with your newly arrived colleague.

Due to your amazing interest in the course topic, you wonder, "What must the horizontal turbulent diffusivity be in the lecture hall?"

PCE Concentration Profiles

Depth z (m)	PCE Concentration (10^{-9} mol L^{-1})	
	June 10	July 10
0	1.0	0.5
2	5.0	2.0
4	9.5	3.5
6	5.5	5.5
8	3.9	4.7
10	3.1	3.6
12	2.6	3.0
14	2.3	2.7
16	2.1	2.4
18	2.0	2.2
20	1.9	2.1

P 17.12 *Vertical Turbulent Diffusivity in a Lake calculated from Measurements of Tetrachloroethene (PCE)*

In a lake with maximum depth of 20 m, two vertical profiles of our companion compound tetrachloroethene (PCE) were measured at a time interval of one month (see table). Calculate the vertical turbulent diffusivity, E_z, at 8, 12, and 16 m depth. As a first estimate, assume that A(z) is constant from the lake surface to the deepest part ("rectangular lake basin"). Assume that PCE does not undergo any reactions in the waterbody. Inputs and outputs are exclusively located at the surface (inlets, outlet, and air–water exchange).

P 17.13 *Radon Profiles and Vertical Turbulent Diffusivity*

Near the bottom of the Hatteras Abyssal Plain in the North Atlantic, several vertical profiles of excess radon-222 activities were measured. The table gives data

from profiles taken on August 6, 1977. Calculate E_z for the lowest 40 m of the water column.

Radon-222 Activities

Distance from bottom h (m)	Activity excess radon (dpm/100 kg) [a]
4	41.6±1.1
11	35.1±3.8
16	30.2±2.0
21	24.7±1.2
27	17.5±1.1
34	12.3±1.8

[a] Activity units: dpm/100 kg = decay per minute per 100 kg of seawater

P 17.14* *Vertical Distribution of Dichlorodifluoromethane (CFC-12) in a Small Lake*

Dichlorodifluoromethane (CCl_2F_2, CFC-12) enters a small lake (surface area $A_o = 2 \times 10^4$ m^2, maximum depth $z_m = 10$ m) from the atmosphere by air–water exchange (see Chapter 19). The top 2 m of the lake is well-mixed. Vertical turbulent diffusion between 2 and 10 m depth is estimated to be $E_z = 1 \times 10^{-5}$ m^2 s^{-1}. Groundwater infiltrates at the bottom of the lake adding fresh water at the rate of $Q_{gw} = 100$ L s^{-1}. The only outlet is at the surface. The CFC-12 concentration in the mixed surface water is $C_o = 10 \times 10^{-12}$ mol L^{-1} and below detection limit in the infiltrating groundwater.

Within the water column, CFC-12 can be considered to be non-reactive. Disregard the dependence of A on depth of the lake when answering the following questions:

(a) Calculate the vertical flux of CFC-12 at 2 and 6 m depth at steady state.

(b) How long would it take for the CFC-12 profile to reach steady state?

(c) Calculate the vertical profile of CFC-12 between 2 and 10 m depth by assuming steady-state conditions, that is, all relevant parameters are constant with time.

dichlorodifluoromethane
(CFC-12)

Hint: The vertical profile can be calculated from a reduced version of the one-dimensional transport-reaction equation (Eq. 6-38) by omitting the first two terms (reaction terms). The remaining two terms describe advective and diffusive transport. Two boundary conditions are needed. One is given by the CFC-12 concentration in the top 2 m of the lake. The key for the second boundary condition (the one for $z = z_m$) is indirectly given by the answer to question (a). The answer to this question does not need any mathematics. Just remember that CFC-12 is neither produced nor degraded in the water column and that the infiltrating groundwater does not contain any CFC-12.

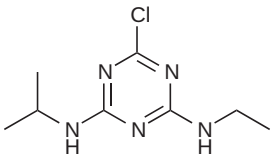

atrazine

River T characteristics

Discharge Q = 50 m^3 s^{-1}
Mean flow velocity
v_x = 0.5 m s^{-1}
Dispersion coefficient
E_{dis} = 50 m^2 s^{-1}

P 17.15* ***An Atrazine Spill in River T***

An unknown amount of the herbicide atrazine is accidentally spilled into River T. Fortunately, the river is a special investigation site of the local water authority, thus all the relevant hydraulic parameters of the river are known. Several water samples were taken about 3.5 km downstream of the place where the accident occurred. The maximal concentration of atrazine was measured in a sample taken exactly one hour after the accident, with a concentration of $C_{max}(t_o = 1 \text{ hour}) = 80\ \mu gL^{-1}$.

(a) 15 km downstream from where the accident occurred is the intake of a local drinking water supply. You were asked whether the pumps should be stopped, and, if yes, how soon. The tolerable drinking water concentration of atrazine is 0.1 μgL^{-1}. For a moment, you believe that the maximum concentration would drop fast enough by the effect of dilution by other rivers further downstream and by dispersion. Then you realize that other rivers do not add more than 20% to the discharge over the next 15 km. With respect of dispersion, you remember Eq. 17-39. What do you tell your colleagues at the water supply plant?

(b) You are curious to estimate the total amount of atrazine that has been spilled into River T. Maybe the samples taken one hour after the accident in combination with Eq. 17-39 would help. To simplify the calculation, you assume that the total mass of atrazine, $\mathcal{M}$, has entered the river within a very short time at one particular location one hour upstream of the site where the first samples were taken.

17.5 Bibliography

Abraham, M. H.; McGowan, J. C., The use of characteristic volumes to measure cavity terms in reversed phase liquid chromatography. *Chromatographia* **1987**, *23*(4), 243–246.

Aminabhavi, T. M.; Naik, H. G., Chemical compatibility study of geomembranes - sorption/desorption, diffusion and swelling phenomena. *J. Hazard. Mater.* **1998**, *60*(2), 175–203.

Boudreau, B. P., The diffusive tortuosity of fine-grained unlithified sediments. *Geochim. Cosmochim. Acta* **1996**, *60*(16), 3139–3142.

Broecker, W. S., An application of natural radon to problems in ocean circulation. In *Diffusion in Oceans and Fresh Waters*, Ichiye, T., Ed. Lamont Doherty Geol. Obs.: Palisades, NY, 1965; pp 116–145.

Carslaw, H. S.; Jaeger, J. C., *Conduction of Heat in Solids*. 2nd ed.; Oxford University Press: Oxford, UK, 1959.

Crank, J., *The Mathematics of Diffusion*. 2nd ed.; Clarendon Press: Oxford, 1975.

Cussler, E. L., *Duffusion: Mass Transfer in Fluid Systems*. 3rd ed.; Cambridge University Press: Cambridge, 2009; p 631.

Einstein, A., Über die von der molekularkinetischen Theorie der Wärme geforderte Bewegung von in ruhenden Flüssigkeiten suspendierten Teilchen. *Annalen der Physik* **1905**, *322*(8), 549–560.

Fischer, H. B.; Imberger, J.; List, E. J.; Koh, R. C. Y.; Brooks, N. H., *Mixing in Inland and Coastal Waters*. Academic Press: New York, 1979.

Floryan, M., Galton Box.svg. Wikicommons: 2007. https://commons.wikimedia.org/wiki/File:Galton_Box.svg.

Fuller, E. N.; Schettle, P. D.; Giddings, J. C., A new method for prediction of binary gas-phase diffusion coeffecients. *Ind. Eng. Chem.* **1966**, *58*(5), 18–27.

Gaiselmann, G.; Neumann, M.; Schmidt, V.; Pecho, O.; Hocker, T.; Holzer, L., Quantitative relationships between microstructure and effective transport properties based on virtual materials testing. *Aiche J.* **2014**, *60*(6), 1983–1999.

Gao, X. C.; da Costa, J. C. D.; Bhatia, S. K., Understanding the diffusional tortuosity of porous materials: An effective medium theory perspective. *Chem. Eng. Sci.* **2014**, *110*, 55–71.

Gargett, A. E., Vertical eddy diffusivity in the ocean interior *J. Mar. Res.* **1984**, *42*(2), 359–393.

Gevao, B.; Harner, T.; Jones, K. C., Sedimentary record of polychlorinated naphthalene concentrations and deposition fluxes in a dated Lake Core. *Environ. Sci. Technol.* **2000**, *34*(1), 33–38.

Hayduk, W.; Laudie, H., Prediction of diffusion coefficients for non-electrolytes in dilute aqueous solutions. *Aiche J.* **1974**, *20*, 611–615.

Hillel, D., *Environmental Soil Physics*. Academic Press, Inc.: San Diego, 1998; p 771.

Imboden, D. M.; Eid, B. S. F.; Joller, T.; Schurter, M.; Wetzel, J., MELIMEX, an experimental heavy metal pollution study: Vertical mixing in a large limno-corral. *Schweiz. Z. Hydrologie* **1979**, *41*(2), 177–189.

Imboden, D. M.; Emerson, S., Natural radon and phosphorus as limnologic tracers: Horizontal and vertical eddy difussion in Greifensee. *Limnol. Oceanogr.* **1978**, *23*(1), 77–90.

Imboden, D. M.; Wüest, A., Mixing mechanisms in lakes. In *Physics and Chemistry of Lakes*, Lerman, A.; Imboden, D. M.; Gat, J. R., Eds. Springer: Berlin, 1995; pp 83–138.

Jeans, J. H., *The Dynamical Theory of Gases*. 3rd ed.; Cambridge University Press: Cambridge, 1921; p 462.

Kawaguchi, Y.; Kikuchi, T.; Inoue, R., Vertical heat transfer based on direct microstructure measurements in the ice-free Pacific-side Arctic Ocean: The role and impact of the Pacific water intrusion. *J. Oceanogr.* **2014**, *70*(4), 343–353.

Knowledge Seeker, Chicago River, dye travelling upstream.jpg. Wikicommona: 2005. https://commons.wikimedia.org/wiki/File:Chicago_River,_dye_travelling_upstream.jpg#file

Lerman, A., *Geochemical Processes: Water and Sediment Environments*. John Wiley and Sons, Inc.: New York, 1979; p 481.

Okubo, A., Oceanic diffusion diagrams. *Deep Sea Res.* **1971**, *18*(8), 789–802.

Osborn, T. R., Estimates of the local rate of vertical diffusion from dissipation measurements. *J. Phys. Oceanogr.* **1980**, *10*(1), 83–89.

Othmer, D. F.; Thakar, M. S., Correlating diffusion coefficients in liquids. *Ind. Eng. Chem.* **1953**, *45*, 589–593.

Quinn, J. A.; Anderson, J. L.; Ho, W. S.; Petzny, W. J., Model pores of molecular dimension. The preparation and characterization of track-etched membranes. *Biophys. J.* **1972**, *12*(8), 990–1007.

Renkin, E. M., Filtration, diffusion, and molecular sieving through porous cellulose membranes. *J. Gen. Physiol.* **1954**, *38*(2), 225–243.

Rutherford, J. C., *River Mixing*. Wiley: Chichester, **1994**; p 347.

Stumberg, J., Petty Officer 2nd Class, Defense.gov photo essay 100506-N-6070S-819.jpg. Wikicommons: 2010. https://commons.wikimedia.org/wiki/File:Defense.gov_photo_essay_100506-N-6070S-819.jpg

Wilke, C. R.; Chang, P., Correlation of diffusion coefficients in dilute solutions. *Aiche J.* **1955**, *1*(2), 264–270.

Witherspoon, P. A.; Bonoli, L., Correlation of diffusion coefficients for paraffin, aromatic, and cycloparaffin hydrocarbons in water. *Ind. Eng. Chem. Fundamen.* **1969**, *8*(3), 589–591.

Yaws, C. L., *Transport Properties of Chemicals and Hydrocarbons: Viscosity, Thermal Conductivity, and Diffusivity of C1 to C100 Organics and Ac to Zr Inorganics*. William Andrew Inc: Norwich, 2009; p 597.